HALL EFFECT MEASUREMENTS OF GROUP II-VI SEMICONDUCTORS

By

MUJTABA IKRAM
2009-NUST-MS Ph.D-MS-E-10

Supervised By
Prof. Dr. ASGHARI MAQSOOD (Sitara-e-Imtiaz)

Co-Supervisor
Dr. N.A. Shah

This work is submitted as a dissertation in partial fulfillment of the requirement for the degree of

MASTERS OF SCIENCE (MS)
In
MATERIALS AND SURFACE ENGINEERING

School of Chemical and Materials Engineering
National University of Sciences and Technology (NUST), H-12, Islamabad, Pakistan

Certificate

This is to certify that the work in this dissertation has been carried out by Mujtaba Ikram and completed under my supervision at Thermal Transport Laboratory, School of Chemical and Materials Engineering, National University of Sciences and Technology, Islamabad, Pakistan

Prof. Dr. Asghari Maqsood (Sitara-e-Imtiaz)

Supervisor

Thermal Transport Laboratory,

School of Chemical and Materials Engineering,

National University of Sciences and Technology,

Islamabad, Pakistan

Dr. N.A.Shah

Co-Supervisor

Department of Physics

COMSATS Institute of Information Technology, Islamabad, Pakistan

Submitted through

Prof. Dr. M. Shahid

Head of Department

O my Rabb (Cherisher and Sustainer)! Bestow wisdom on me, and join me with the righteous; grant me honorable mention on the tongue of truth among the latest (generations); make me one of the inheritors of the Garden of Bliss." Al-Quran (26:83-84)

ACKNOWLEDGEMENTS

All Praises to Almighty Allah, the Lord of the entire universe. With Your prolific praise, O Owner of Honors, I desire to begin. A limitless praise, with which You are Pleased. It is undeniable that all manifestation of nature bears eloquent testimony to the fact that Allah is the creator, the Maintainer and the Regulator of the world. He makes Laws for the evaluations of things and sets them on the path of perfection. Almighty Allah who bestows and blesses knowledge, technology and scientific ingenuity to man through experimental research and remarkable deduction to ponder over the forces of nature. In the first place, therefore, we express our utmost thanks to Almighty Allah the omnipresent and the creator of the worlds, who has endowed us brain and instable instinct construction of knowledge and body to accomplish our work in the form of this plant report.

I offer my great and best gratitude to the last Prophet MUHAMMAD (S.A.W), who has given the lesson of altruism, generosity, benevolence and moral values and also broke the cage of servitude through His golden sayings, to seek knowledge is obligatory for every Muslims.

I express my sincere thanks to my respected supervisor Meritorious Prof Dr. Asghari Maqsood for her worthy guidance in preparing this report and her kind and valuable supervision on all the practical work performed. I have always looked up to her for guidance in any problem I faced in my work and I consider myself privileged to work under her supervision which always prove to me with cogent vision of exploring things and ideas.

I greatly acknowledge Prof Dr. Mohammad Mujahid, Principal School of Chemical and Materials Engineering (SCME), NUST for providing a platform to utilize my skills in the research work. I would like to thank all the faculty members, non-teaching staff and my fellow students for the help provided to me at various stages during this research work.

My deep appreciation and a bundle of eloquent and perspicacious thanks for Prof. Dr. Mohammad Shahid, head of Materials Engineering department, SCME for his sincere and inspiring guidance.

I acknowledge M. Umer Farooq, Imran and Shahid Ameer for their support during my research work. I am also thankful to Zafar Iqbal for his technical support during my all research work. I am really grateful to other laboratory fellows for their help in various stages of experimentation during my research work. I acknowledge Higher Education Commission and School of Chemical and Materials Engineering (SCME), NUST, Pakistan, for the technical and financial assistance provided through HEC Project 694 during my research.

I may thanks Adnan Nazir, Shahzad Salam, Majid Khan and Asif Mahmood for useful and valuable discussion during my research work. I am grateful to all my class fellows and friends especially Hassan Younas, Adil, Sibghatullah, Usman Tahir, Tahir Mahmood, Zohaib Khan, Aftab Akram and Sajid Riaz being the surrogate family at NUST and for providing the unforgettable company.

Last but not least I would like to thank my Parents and all other family members for their motivational support, without their confidence in me and support this work would have never been accomplished.

Mujtaba Ikram

Dedicated to My loving Parents, caring Uncle Qazi Abdul Khaliq, my Fiancee and affable Family who always inspired me to explore Ideas of Life with modest vision and foster me through odd and even situations of Life

Table of Contents

TABLE OF FIGURES

Chapter 1

Chapter 2

Chapter 3

Chapter 4

LIST OF TABLES

Hall Effect measurements of II-VI group semiconductors

Mujtaba Ikram, Thermal Transport Laboratory, SCME, NUST, Islamabad, Pakistan

ABSTRACT

In the present work, "Ecopia 5000 Hall effect measurements system", has been made operational successfully for the first time at Thermal Transport Laboratory, SCME, NUST, Islamabad. Electrical characterization of ZnO and CdS thin films has been done with the help of Ecopia 5000 Hall Effect measurement system. ZnO and CdS thin films have been prepared by sol gel and close space sublimation techniques. These films were characterized by SEM, XRD, EDS and Hall Effect measurement for their morphological, structural, and electrical properties respectively. The electrical resistivity's of ZnO and CdS thin films were found to be of order of 10^3 and 10^5 ohm-cm respectively. Decreasing trend for magneto resistance as a function of temperature was also observed for both ZnO and CdS films. The change in the resistivity of these materials was about 2% of the order in the change of resistivity when these films were subjected to magnetic field of 0.55 T which confirmed anisotropic magneto resistance phenomenon in both of these semiconductor films. Resistivity and sheet resistance variations with thickness were also determined for these films. In ZnO and CdS thin films, as thickness and temperature increased the resistivity of both of these films decreased which confirmed semiconductor like behavior. I-V characterizations for these films under light and dark conditions showed features which is responsible for its applications as photovoltaic materials. The resistivity of ZnO and CdS thin films has followed the hopping model which also confirmed the semiconductor like nature of these thin films. As for ZnO and CdS films, hopping distance decreased while hopping energy increased linearly with rising temperature. Both these films have followed necessary conditions for Mott's VRH mechanism. The said model is applied to dc electrical resistivity data.

CHAPTER 1

1.0 Introduction

The purpose of this research project includes 1) to learn about the Hall effect measurement technique to find out the carrier density, resistivity, magneto resistance, sheet resistance and mobility in semiconductors and metal thin films, (2) to establish various Hall-related phenomena, (3) to show various application of the Hall effect phenomena [1], and (4) to set off a discussion based upon electronic interaction where workers involved in this phenomena can exchange and discuss ideas, information and new scientific concepts. The following detail will lead us through an introductory sketch of the Hall measurement, covering basic aspects and principles, equipment, and some suggested procedures. Then this is followed by some brief conversation of phenomena which is basically related to the Hall effect. Some wide applications of the Hall effect in industrial and consumer products are also discussed.

1.1 Importance of Hall Effect

The importance and significance of the Hall effect is supported by the necessitate to find out accurately carrier concentration, dc electrical resistivity, mobility, Hall coefficient and sheet magneto resistance in case of metals and semiconductors thin films, which account basically in electrical characterization of these thin surface coatings . This Hall effect is basically a relatively very simple method for doing all these measurements.

1.2 Vital characterization technique in the semiconductor industry

Some of valuable features of Hall effect measurements systems show that it is an indispensable and vital technique for semi conductor industry and for different research laboratories. These features include as simplicity of apparatus followed by accurate turnaround time and very acceptable low cast. Because of such amazing features of Hall effect, this also include one of the most commonly used characterization tools. Two Noble prizes in 1985 and 1998 are based upon this valuable technique.

1.3 History behind this Concept

The narration of the Hall effect started by Edwin H. Hall in 1879 when Edwin H. Hall concealed that a meaningful small transverse voltage formed across a current-carrying thin metal strip when it was subjected to an applied magnetic field. Until that time, electrical measurements provided only the some basic parameters like carrier density-mobility product, so as a consequence the partition of these two important objective physical quantities had to be dependent on other complicated and difficult measurements. The concepts of the Hall effect gave an establish relation which was basically a straight and direct measure of the carrier density. The polarity of this transverse Hall voltage also proved valuable information about electrons that these are physically moving in an electric current which is basically related to the flow of charges. The advancement of this Hall effect technique has led to a formation of a mature, practical and multi-featured tool, which today is widely used in semi conductors industry and for characterizing the electrical properties of metals and semi conductor's thin films throughout the world.

1.4 The Hall Effect

1.4.1 From where resistance concepts came?

Electrical characterization of semi conductors' materials basically involved in different levels of perceptive and understanding. In the time span of early 1800s, the two important quantities as resistance (R) and conductance (G) were been treated as measurable physical parameters which obtained from two-terminal I-V measurements, I stands for current and V stands for voltage. Later on, it became understandable that the quantity resistance alone was not enough broad because of different sample shapes and geometries gave different values for resistance. As a consequence of this, it led to the understanding of next level. According to which, resistivity (which is inverse of conductivity) is supposed to be an important intrinsic material property. Amazing feature of resistivity is that it is not influenced by any

specific geometry or shape of the sample. After valuable understanding of intrinsic material property, this gave scientists a new vision to quantify the current-carrying ability of the material and then as a result of that, it corresponded to accomplish meaningful and important comparisons between different types of materials.

1.4.2 Evolution of concepts about carrier density and mobility

In the span of early 20^{th} century, it was observed that resistivity was not a more fundamental and basic material parameter, the solid reasoning behind was that different materials can comprise the same order of resistivity values. On the other hand, a given material can have different values of resistivity depending upon the method of synthesis. This factor came true especially in case of semi conductor materials, so in case of semi conductors' resistivity alone was not enough for complete electrical studies. So as a solution of this problem, theories of electrical conduction were introduced with reliable degrees of accomplishment, but after rise of theories of quantum mechanics, not any general acceptable and reliable solution to the problem of electrical transport was developed. This led scientist to the new level of understanding which accomplish with concepts of carrier density n and carrier mobility μ ,so this all helps a lot to deal with even most complex electrical measurements.

1.4.3 The concept of Lorentz Force

Lorentz force is the basic physical principle that covers the Hall effect [2]. Lorentz force is basically a combination of two separate forces; these forces include the electric as well as the magnetic force. Suppose an electron moving along the direction of electric field which is perpendicular to an applied magnetic field, then it experiences a force which is magnetic force represented as -qV X B which is acting normal to both the directions. If one is interested in knowing the direction of this magnetic force then it can be determined with the help of right hand rule. Figure 1.1 shows the concepts of Lorentz force.

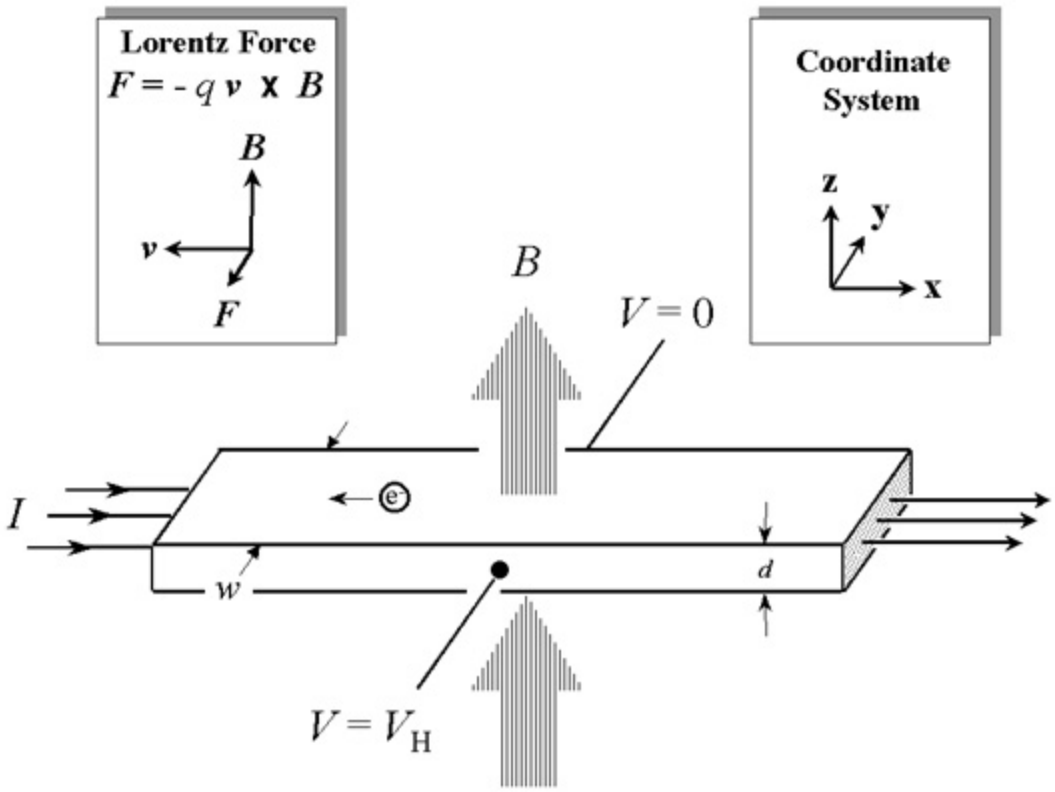

Figure 1.1: Concept of Lorentz force

1.4.4 Right hand rule for direction

Right hand rule for direction of magnetic force states with an open hand, the fingers are pointed along the direction of the carrier velocity and curled into the direction of the magnetic field [3]. The opposite direction that the thumb is basically pointing is the direction for magnetic force actually on an electron. Expression for this Lorentz force F is therefore determined by the mathematical relation as - q(E + v x B) where q is elementary charge and the value for q is 1.602×10^{-19} Coulomb, E stands for electric field, v for particle velocity, and B stands for the magnetic field applied.

1.4.5 Hall Voltage

Let us suppose we have bar-shaped semiconductor thin film [4] such as shown in Figure 1.1, this thin film is n-type semi conductor. If it is n-type semi conductor then carriers are predominately electrons not holes with bulk density n. Suppose that a current of constant magnitude I flows along the x-axis from one side to another side in other words from left to right but in the presence of a magnetic field which is z-directed magnetic field. Electrons in case of semi conductor thin film which are subjected to some force which is basically Lorentz force results in initial drifting away from the direction of current towards the negative y-axis, as a consequence of this drifting there is an excess of negative surface electrical charges on this side of the sample in comparison with the other side of the same sample. So there must be difference of potential on both sides of the sample which results in the form of Hall voltage, which is basically a potential drop across the two sides of the sample. On the other hand, the force on holes is obviously toward the same side, reason is that holes have opposite velocity and opposite charges i.e. positive charges. This transverse voltage is termed as Hall voltage V_H and mathematically V_H is equal to

$$V_H = IB/qnd \qquad (1.1)$$

Where d stands for thickness of the thin film sample, B, I and q are already defined and n is for density of charge carriers.

1.4.6 Sheet density n_s

For using sheet or layer density we have this relation as $n_s = nd$ where n_s is sheet density and n is bulk density if we use sheet density instead of bulk density then equation (1.1) has reduces to

$$n_s = IB/q|V_H| \qquad (1.2)$$

One can measure the Hall voltage V_H from equation (1.1) and then from equation (1.2) with the help of known values of current, magnetic field and elementary charge, one can easily find out the sheet density n_s of charge carriers in case of semiconductors thin films.

1.4.7 Identification between n-type and p-type semi conductors

For n-type semiconductors, Hall voltage is negative. And it should be positive for semiconductors of p-type.

1.4.8 Sheet resistance

Van der Pauw resistivity measurement technique can be used to find out the sheet resistance R_S of the semiconductor.

1.4.9 Hall mobility

As sheet resistance involves with both mobility and sheet density, Hall mobility can be easily calculated from the equation (1.3) which state as

$\mu = |V_H|/R_S IB = 1/(qn_S R_S)$ (1.3).

1.4.10 Bulk resistivity and bulk density

If one has knowledge about the thickness of the thin film then bulk resistivity and bulk density can be easily estimated from the equation (1.4) and equation (1.5) which stated as

$r = R_S d$(for bulk resistivity) (1.4)

$n = n_S/d$ (the bulk density) (1.5)

1.4.11 Bulk conductivity

Conductivity is reciprocal of resistivity. If one knows about the bulk resistivity then one can easily determined about the bulk conductivity as well.

1.4.12 Magneto resistance

Magneto resistance is the property of a material which deals with the change of resistivity of material when it is subjected to magnetic field. Different materials show different type of magneto resistance effects which depends upon how much the change in the resistivity occurs when materials are subjected to magnetic field. Magneto resistance is classified [5] as

- ✓ Ordinary Magneto resistance
- ✓ Anisotropic Magneto resistance
- ✓ Giant Magneto resistance
- ✓ Colossal Magneto resistance

In case of non-magnetic metals, effect of magneto resistance is supposed to be very low with low fields and the effect can become quite large with high fields. The variation in resistivity is positive either in case of magnetic field parallel to current direction or magnetic field transverse to current direction but with condition i.e. resistivity at transverse magnetic field > resistivity at parallel magnetic field. So the change in resistivity is positive for both parallel and transverse magnetic fields in case of ordinary magneto resistance. This behavior can observe in different metals like Al, Cu, Zn and Na etc. Anisotropic magneto resistance can be observed in different ferromagnetic alloys and metals at room temperature. If change in resistivity at room temperature is of order of 2% at low fields then it will correspond to the case of anisotropic magneto resistance. In case of anisotropic magneto resistance, change in resistivity when it is applied with parallel magnetic field increases with field and change in resistivity when it is applied with transverse magnetic field decreases with field. At low temperature, magneto resistance is found to be occurring in case of system of multilayer magnetic films. Giant magneto resistance is observed in anti-ferromagnetically coupled multilayers of Fe/Cr. Such structure contains thin layers of magnetic metals which are separated by different non-magnetic metals layers. In case of configuration for anti-ferromagnetic or ferromagnetic, the magnetic layers are coupled through non-magnetic layers. Such coupling depends upon thickness of non magnetic layers. So magneto resistance

effect in this case is up to ~50% at low temperature. Colossal magneto resistance is very new concept in studies of magneto resistance. This type of magneto resistance is observed in perovskite structures. So the change of resistivity in case of colossal magneto resistance is found up to 99.9%.

1.5 The Van der Pauw Technique

The determination of the sheet density and mobility require both the Hall measurement and resistivity measurement [6]. For the measurements of resistivity of uniform samples, Van der Pauw technique is widely used for this purpose [7]. This technique for measurements of resistivity originally introduced by Van der Pauw. For this measurement, one uses an arbitrary shaped and thin-plate sample and characteristics of such sample includes no holes and no inclusions or non conducting islands. At the four corners of such thin-plate sample, very small ohmic contacts should locate. Figure 1.2shows a good configuration for rectangular sample used for Van deer Paw technique.

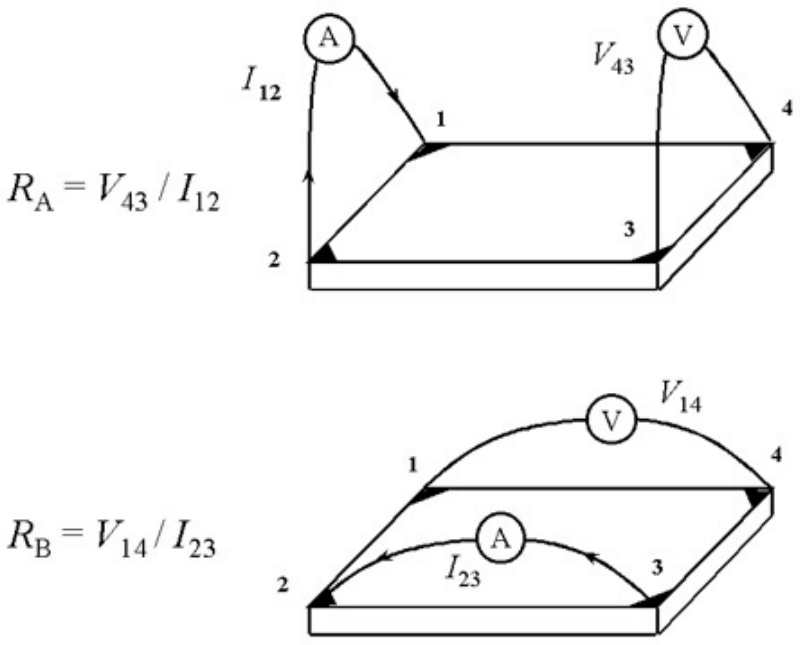

Figure 1.2: Configuration of sample for Van der Pauw technique

1.5.1 Determination of Characteristics Resistances via Van der Pauw technique

To find out the sheet resistance R_S of the sample is basically the main goal of the resistivity measurement. There are two characteristics resistances i.e. R_A and R_B which were established by Van der Pauw. Both resistances R_A and R_B are linked with the consequent terminals as also shown in Figure 1.2. As we have a van der pauw equation so both characteristics resistances i.e. R_A and R_B are correlated to the sheet resistance R_S via Van der Pauw equation. This Van der Pauw equation is stated below

$$\exp(-\rho R_A/R_S) + \exp(-\rho R_B/R_S) = 1 \quad (1.6)$$

Equation (1.6) can be solved numerically. Such numerical solution of Van der Pauw equation gives sheet resistance R_S.

If one measures the sheet resistance with the help of Van der Pauw equation then one can easily estimate the bulk resistivity of thin-plate sample as well as the thickness of thin-plate sample following equation (1.7)

$\rho = R_S d$ (1.7)

For measurement of characteristic resistance R_A, one applies dc current I_{12}which flows into the contact first and out of contact second and then measures the voltage V_{43} from contact fourth to contact third. Then for the measurement of second characteristics resistance R_B, one applies the dc current which flow into the contact second and out of contact forth and then measures the voltage V_{14} which correspond I.e. contact first to contact fourth. So then both characteristics resistances R_A and R_B are measured with help of following expressions (1.8) and (1.9) are as follows

$R_A = V_{43}/I_{12}$ (1.8)

$R_B = V_{14}/I_{23}$ (1.9)

1.5.2 Sheet density by Van der Pauw technique

To measure sheet carrier density n_s by means of Hall voltage V_H is one of the intentions of the Hall measurement in the Van der Pauwmethod [8]. Measurement for Hall voltage corresponds to a series of voltage measurements with constant values of current and magnetic field applied at right angles to the plane of the thin-plate sample. Suppose the same thin-plate sample for the measurements of hall voltage as shown in Figure 1.3.

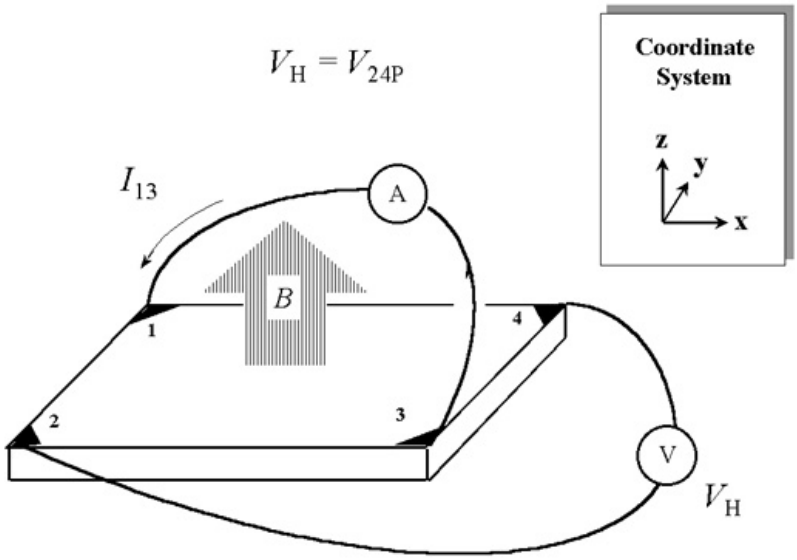

Figure 1.3: Thin plate sample for hall voltage

Hall voltage V_H can be measured when a current is forced through the opposite pair of contacts i.e. first and third and then the Hall voltage V_H (must have relation with V_{24} asV_H=V_{24}) is calculated across the remaining pair of contacts i.e. second and fourth. When one has calculated this Hall voltage then the sheet carrier density n_s can be easily calculated with equation (1.2) after knowing the other parameters of equation (1.2).

1.5.3 Van der Pauw technique in case of irregular shape sample

Some samples have irregular shapes. Irregular shape means which are not square or rectangular type. For such irregular samples like bridge type or parallelepiped sample as for anisotropic material properties, the limitations on size of sample as well of its shape are more rigid than those of the Van der Pauw sample, but keeping in mind such measurements can be completed using a different contact configurations [8] like eight or six configuration of contacts. There is difference in placement of contacts in both bridge-type and parallelepiped samples. For example bridge-type sample differs from the parallelepiped in that the contacts are placed on arms instead of corners that also branch off the main parallelepiped base.

1.6 Considerable practical aspects

Some considerable practical aspects while doing resistivity and hall measurement are observed. These aspects relate to ohmic contact and size and quality of ohmic contact, determination of thickness and uniformity of sample, thermo magnetic effects which occur due to non uniformity of temperature, and photovoltaic and photoconductive effects. Measurements in dark conditions reduce photovoltaic and photoconductive effects. One of most important condition for measurement is that sample lateral dimensions should large in comparison with size of the contacts and as well with the thickness of sample. After first condition satisfied, one can easily measure magnetic field intensity, temperature of sample, voltage and current.

1.7 Shape of thin-plate Sample

For hall measurements, one needs a fabrication of thin-plate semi conductor sample such that it should adopt a suitable geometry as shown in Figure 1.4. So for such suitable sample, the thickness (d) of sample and the average diameters (D) of the contacts should be smaller in comparison with the distance between the contacts (L). Relative errors should be of the order of D/L i.e. these relative errors are caused by some values of D which are non-zero. Sample shape in figure (a) is preferred for hall measurement. On other hand, square shape of sample in figure (b) is acceptable and reliable and contacts at the edge or within perimeter of a sample are not recommended at all as in figure (c). Contacts at corners of sample are very acceptable but the contacts at edges are not acceptable.

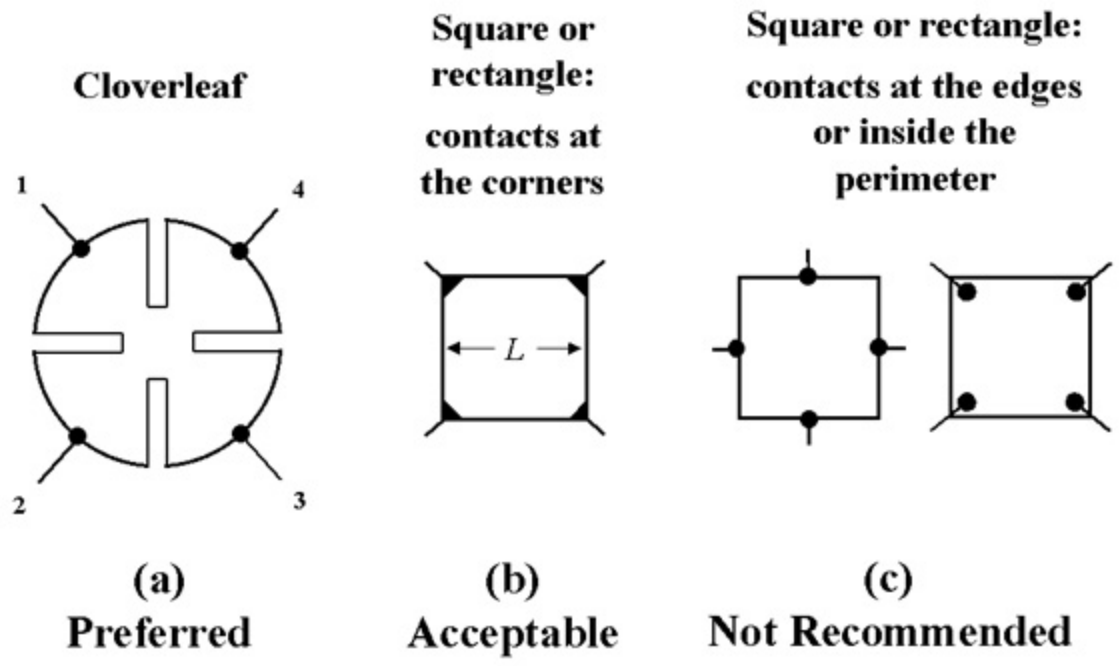

Figure 1.4: Different geometries of sample

1.8 How to make Resistivity Measurements?

For the possibility of resistivity measurement, four probes are connected to the four contacts of the sample, contacts preferably should be ohmic. One can easily label these ohmic contacts as 1, 2, 3, and 4 which turn counterclockwise as shown in Figure1.4 (a). To reduce the thermo electric effects, one should use same type of wires of probes which should connected to ohmic contacts but keep in mind all contacts should be of the same material. One has to define some parameters like thickness of sample, sample resistivity and current flow through different contacts so suppose

ρ = resistivity of sample taken in Ω-cm

d= thickness of conducting layer taken in cm and I_{12} is a positive dc current which is injected into first contact and then taken out of contact second, similarly for different currents between different contacts I.e.I_{23}, I_{41}, I_{14}, I_{43}, I_{32},I_{34}, I_{21}. All currents are taken in

Amperes.$V_{12}$is dc voltage which measured between two different contacts i.e. first and second and is equal to V_1 - V_2which is without applying any magnetic field so in this case B is taken as zero. Similarly for different voltages between different contacts i.e.V_{23}, V_{41}, V_{14}, V_{43},V_{34},V_{32} and V_{21}. All voltages are taken in volts.

1.8.1 Important features and relations for resistivity measurements

Here are some different calculations which relate to resistivity measurement. For quality of ohmic contact, internal consistency, and for sample uniformity, data should be checked. So establish a dc current and when this dc current is applied to the sample then the power dissipation does not exceed 5 mW, preferably it should be 1 mW. This boundary can be precise before the automatic measurement sequence is started by measurement of the resistance R between any two opposing probes either first to third or second to fourth and by setting a condition i.e. $I< (200R)^{-0.5}$. For measuring voltage V_{34}, one should apply the current I_{21} and similarly for V_{43}, one should apply current I_{12}. Similarly measure the other all voltages between different contacts i.e. V_{41}, V_{14},V_{21},V_{12}, V_{32},V_{23}. Eight values of resistances are calculated with help of corresponding eight voltages as all of which should be positive and express as shown in combined equation (1.10)

$$\begin{aligned} R_{21,34} &= V_{34}/I_{21},\ R_{12,43} = V_{43}/I_{12}, \\ R_{32,41} &= V_{41}/I_{32},\ R_{23,14} = V_{14}/I_{23}, \\ R_{43,12} &= V_{12}/I_{43},\ R_{34,21} = V_{21}/I_{34}, \\ R_{14,23} &= V_{23}/I_{14},\ R_{41,32} = V_{32}/I_{41}. \end{aligned} \qquad (1.10)$$

For the consistency of measurement, it should follow the current reversal which requires as shown in combined equation (1.11)

$$\begin{aligned} R_{21,34} &= R_{12,43}, \\ R_{43,12} &= R_{34,21} \\ R_{32,41} &= R_{23,14}, \\ R_{14,23} &= R_{41,32} \end{aligned} \qquad (1.11)$$

The reciprocal theorem should be applicable as shown in combined equation (1.12)

$$\begin{aligned} R_{21,34}+R_{12,43} &= R_{43,12}+R_{34,21}, \\ R_{32,41}+R_{23,14} &= R_{14,23}+R_{41,32}. \end{aligned} \qquad (1.12)$$

From above mentioned features if any one of those would fail then one should investigate the sources of error. With the help of two characteristics resistances, one can easily determined the sheet resistance R_S. As characteristics resistances R_A and R_B are express in combined equation (1.13) as

$$R_A = (R_{21,34} + R_{12,43} + R_{43,12} + R_{34,21})/4 \qquad (1.13)$$

$$R_B = (R_{32,41} + R_{23,14} + R_{14,23} + R_{41,32})/4$$

From the numerical solution of equation (1.6), sheet resistance can be easily determined. If one has knowledge about the thickness of the conducting layer, then the bulk resistivity i.e. $\rho = R_S d$ can be easily calculated from value of sheet resistance.

1.9 How to make Hall Measurements?

Magnetic field is essential for doing the Hall measurement [9]. Hall measurements yield the bulk carrier density n or p and the sheet carrier density n_s if one has knowledge about the thickness of sample. As n stand for n-type and p stand for p-type semi conductor materials. Hall voltage of the order of mili-volts i.e. quite small voltage can be find out for thick and heavily doped samples. A type of severe problem has observed from the large offset value of voltage which is due to many factors like shape of specimen, non uniform temperature, and non-symmetric contact placement. The solution of this problem based upon of acquiring two sets of Hall measurements, from these two sets one is used for positive magnetic field direction and second one is used for negative magnetic field direction. The relevant direction is shown in Figure 1.3. I_{13} is the dc current which is injected into lead first and then taken out of lead third. Similarly one can calculate currents for I_{31}, I_{42}, I_{24}between different contacts. B stand for uniform and constant magnetic field intensity which applied parallel to the z-axis within a very few degrees as also shown in Figure 1.3. B can be positive or negative depending upon either it is pointing in positive z-direction or negative z-direction. If it is pointing in positive z-direction then B is positive, when it is pointing in the negative z-direction then B is negative. $V_{24}$is the Hall voltage which measured between different leads i.e. second and fourth with positive magnetic field for current I_{13}. Similarly others measurements can be done likewise for V_{13P}, $V_{42P}$and V_{31P}. Same calculations are also done

i.e. V_{24N},V_{13N},V_{31N} and V_{42}, when magnetic field is reversed or in other words when negative magnetic field is applied.

1.9.1 Important feature and relation for Hall Measurements

For the Hall measurement, one should follow these steps. First of all apply a positive magnetic field B and then apply a current I_{13}, which flows between lead first and lead third and then calculate the voltage across lead second and fourth i.e. V_{24P}. Similarly one can measure theV_{42P} by flowing current through I_{31P}. And then one can estimate the other parametersV_{13P} and V_{31P}as well with flow of current throughI_{42} and $I_{24.}$ Now reverse the magnetic field and applied the negative magnetic field. After applying the negative magnetic field, do measure of V_{24N}, V_{42N}, V_{13N}, and V_{31N} with I_{13}, I_{31}, I_{42}, and I_{24} for the case of negative magnetic field. Sample type either p-type or n-type and the sheet carrier density n_s are determined with the help of different eight measurements of Hall voltages i.e.V_{24P}, V_{42P}, V_{13P}, V_{31P}, V_{24N}, V_{42N}, V_{13N}, and V_{31N}. Equation (1.3) can be used to measure the Hall mobility from the sheet resistance R_S and the sheet density ns. Keep in mind the average Hall voltage calculated from each of the two diagonal sets of contacts must be the same. One has to follow following Steps for the measurements of hall mobility and carrier density. First of all calculate V_F, $VE_{,}$ V_D and V_C with the help of following equations (1.14)

$$V_C = V_{24P} - V_{24N},\ V_D = V_{42P} - V_{42N}, \qquad (1.14)$$

$$V_E = V_{13P} - V_{13N},\ V_F = V_{31P} - V_{31N}.$$

If the polarity of voltage sum $V_C + V_D + V_E + V_F$ is positive then sample is p-type semi conductor and if it is negative then sample is n-type semi conductor. For calculating the sheet carrier density, there are two cases. These cases are

$$p_s = 8x10^{-8}IB/[q(V_C+V_D+V_E+V_F)]$$

if the sum of voltages is positive, or

$$n_s = |8x10\text{-}8IB/[q(V_C+V_D+V_E+V_F)]|$$

if the sum of voltages is negative

Where B stand for magnetic field which is in gauss (G) and I stand for the dc current which is in amperes (A).

For calculation of the bulk carrier density having units of cm^{-3}, one should know the thickness of sample so for n-type or p-type material [10] follows the combined equation (1.15) for bulk carrier density as

$n=n_s/d$

$p = p_s/d$ (1.15)

The Hall mobility can be calculated with help of sheet resistance and sheet carrier density as also stated in equation (1.3).

1.10 Hall Measurement System strengths

As Resistance and conductance were used for electrical characterization in the early span of 1800's, but these properties are widely influence by geometry of sample and also these were not material properties. In order to make comparison between different types of samples with different geometries, some values of resistivity and conductivity were used. These were not even material properties. Strengths of Hall Effect allow measurement of carrier density and mobility, these both basically are material properties [14], and study of these properties always gives a deeper level of understanding of materials**.** The advantages which make hall effect strengthen [15] characterization technique includes low-cost technique, fast turn-around time, Highly sensitivity and even can easily measure carrier concentrations in doped silicon of $<10^{12}$ e-/cm^3.

1.10.1 Hall Measurement System Limitations

There are some limitation about sample geometry, contacts and relate to some photovoltaic effects. These limitations are as follows [15]

- Sample geometry:
  - uniformity of sample
  - Accurate determination of thickness
  - Lateral dimensions should be large compared to sample thickness and contact size
- Ohmic contacts:

– Symmetric placement of contacts on sample
– Size
– Quality
• Thermo magnetic effects
• Photoconductive and photovoltaic effects.

1.10.2 Technological applications of Hall effect

Hall effect sensors are widely used for sensing motion, position, magnetic fields fluid flow, pressure and power. One of hall effect current sensor are shown in figure 1.5.

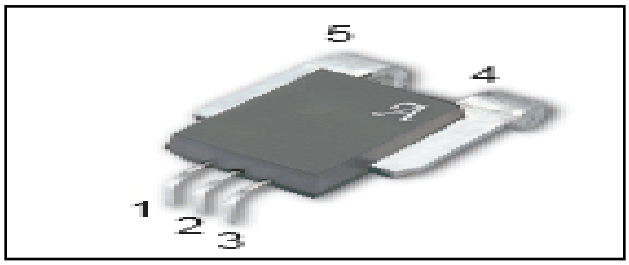

Figure 1.5: Hall effect current sensor

Here are some general properties of Hall effect sensors [11] include as

– Hall effect sensor has long life (30 billion operations, in some tests)
– These sensors are high speed operation (> 100 kHz possible)
– Highly repeatable operation
– Stationary operation (no moving parts)
– Compatible input/output for logic devices

Hall effect has also commercial and Industrial applications [12]. In Electronics industry, Hall effect has a lot of application like Manufacturing low-noise transistors and electronic compasses, In Automobile Industry, it has wide application in fuel injection systems and anti-lock brake systems. In Computers industry, Brushless DC rotors and disk-drive index sensors are include as application of Hall effect. In general, Hydraulic controls Integration

into magnetic shields to reduce stray fields, Inspect tubing or pipelines for corrosion or pitting are include as application of Hall effect [13].

1.11 Materials used in this research

Main focus of this research is on electrical characterization of II-VI semiconductors materials. These materials are synthesized using elements from group second and sixth of periodic table. These semiconductors materials include CdS, CdSe, ZnO, CdTe and ZnS etc. These compound semiconductors do not exist naturally; these are all synthesized in lab. These semiconductors include usually both n-type and p-type materials. CdS and ZnO are studied electrically in this research work.

1.12 References

[1] E. H. Putley, The Hall effect and related phenomena, Butterworths, London (1960).

[2] E. H. Hall, "On a new action of the magnet on electrical current," Amer. J. Math. 2, 287-292 (1879).

[3] D. C. Look, Electrical characterization of GaAs materials and devices, John Wiley & Sons, Chichester (1989).

[4] D. K. Schroder, Semiconductor material and device characterization, 2nd Edition, John Wiley & Sons, New York (1998).

[5] Magneto Resistance Overview: Janice Nickel, Computer Peripherals Laboratory HPL-95-60, June,1995.

[6] L. J. van der Pauw, "A method of measuring specific resistivity and Hall effect of discs of arbitrary shapes," Philips Res. Repts. 13, 1-9 (1958).

[7] L. J. van der Pauw, "A method of measuring the resistivity and Hall coefficient on lamellae of arbitrary shape," Philips Tech. Rev. 20, 220-224 (1958).

[8] R. Chwang, B. J. Smith and C. R. Crowell, "Contact size effects on the Van der Pauw method for resistivity and Hall coefficient measurement," Solid-State Electronics 17, 1217-1227 (1974).

[9] D. L. Rode, C. M. Wolfe and G. E. Stillman, "Magnetic-field dependence of the Hall factor for isotropic media," J. Appl. Phys. 54, 10-13 (1983).

[10] D. L. Rode, "Low-field electron transport," semiconductors & semimetals 10, 1-89 (1975).

[11] Ramsden, Edward, Hall-effect sensors theory and application. 2nd edition.Elsevier, 2006.

[12] “Hall effect sensing and application” Honeywell, Microsensing and Control.

[13] Bridge technology: http://www.four-point-probes.com/ecopia

[14] Hummel, Rolf. E. Electronic properties of materials. 3rd edition. New York: Springer, 2001.

[15] "Hall effect measurements." National institute of standards and technology electronics and electrical engineering laboratory semiconductor materials division. 14 August 2007. U.S. commerce department. 13 november 2007.

CHAPTER 2

2.0 Significance of HMS-5000 Hall Effect Measurement System

The HMS-5000 Hall Effect Measurement System gives us enough data for plotting different graphs i.e. concentration, resistivity, mobility, conductivity and Hall coefficient as a function of temperature. This is the beauty of this apparatus that it can operate at low as well as at high temperature. One can get data in tabular and graph form as well with the help of this apparatus. One can electrically characterize the sample under the temperature range of 80K to 350K. The beauty of this apparatus is that measurements are done automatically without intervention of user. First filling the two reservoirs of LN2 (liquid nitrogen), and then after filling the system automatically applies and switches the input values of current, and then automatically measures the corresponding voltages, temperature variation, and also allow the movement of the magnets automatically which is essential for hall measurements. For HMS-5000 Hall Effect Measurement System, the movement of magnet is totally motor controlled with temperature capability of variable nature, and then powerful software analysis our sample's electrical properties. Without user intervention, theHMS-5000 Hall Effect Measurement System is automatically rise to each temperature which is defined by user, and easily stabilizes, and then make the suitable measurement even with those measurements which include the movements of the magnet automatically. And as a result of Hall measurements by this system one can get various plots which show a diversity of electrical properties of materials which are temperature dependent actually.

2.1 Specifications of HMS-5000 Hall Effect Measurement System

Specifications of the HMS-5000 Hall Effect Measurement System include varsity of features which include as

- Sample size should be of dimension i.e. 5 mm x 5mm up to 15mm x 15mm which is requiring for electrical characterization.

.

- Magnet used in this system is Permanent magnet with diameter of 30 mm.
- Resistivity of sample which has to be measured, must in the range of 10^{-4} to 10^{7} with units Ohms-cm.
- 0.55Tesla is Magnet Flux Density with nominal +/-1% of this marked value for the magnet used in this measurement system.
- Mobility with unit cm2/Volt-sec should be in range of $1 \sim 10^{7}$ for samples which have to be electrically characterized in this system.
- Concentration should be in range of $10^{7} \sim 10^{21}$cm-3 for samples which have to be characterized electrically in this system.
- This hall measurement system has current Source which Ranges from 1nA-20mA and with compliance of 12V
- Minimum value of Hall Voltage should be 1μV for this system.
- Temperature Range for characterizing the sample is 80K to 350K for this hall measurement system.

2.2 General portrayal of HMS-5000 Hall Effect Measurement System

HMS5000 Hall effect measurement system chiefly consists of three main parts which include "Main body System", and "Kit of magnet and Variable controlling system for temperature" and then the "software program" as also portrayed in Figure 2.1.

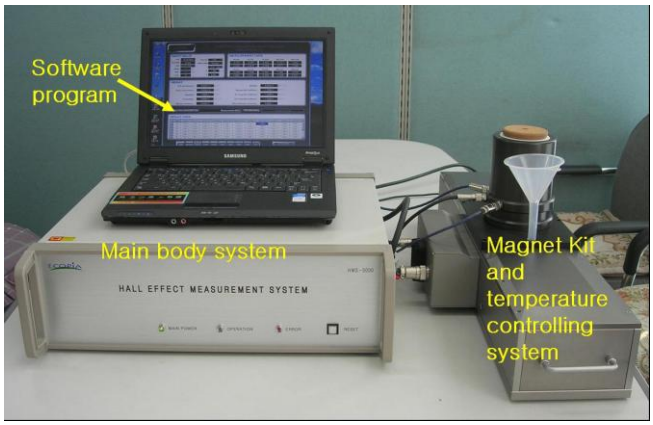

Figure 2.1: HMS5000 Hall effect measurement system

2.2.1 Cables precautions require for Apparatus

One must need to do some precautionary measures for making some characterization on this apparatus. Basics precautions relate to connect all cables correctly as also shown in Figure 2.2.

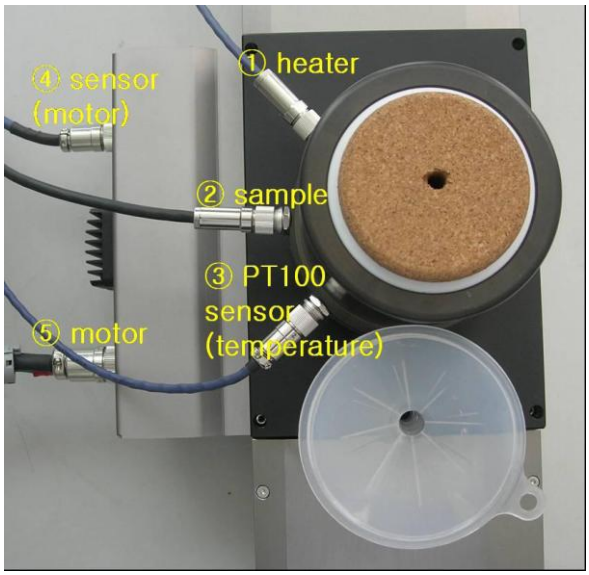

Figure 2.2: Different parts of Hall measurement system

Keep in mind that one side of our first, second and third cables are water proof and the other sides of same cables are not water proof. One can find out which side of cables either are water proof or non-water proof depending upon the length of connectors as water proof connectors are supposed to be little longer in comparison with the connectors of other side. Because of more safety issue, one would prefer to use wafer-proof connectors for connecting to LN2 tank. Reason behind that surface of liquid nitrogen tank will be dewy, while measuring in low temperature [1]. Description for Main body back panel is also shown in Figure 2.3.

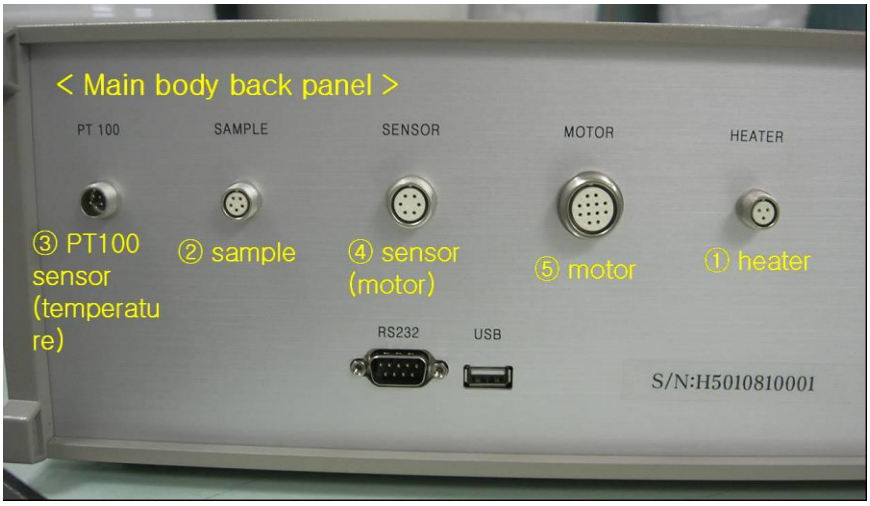

Figure 2.3: Main body back panel

RS232 or USB cable must have connection. This connection comes between connector of back panel of main body system and the computer. Depending upon electrical requirement, the voltage rate switch should be selected. Correct connections for cable configurations are shown in Figure 2.4.

Figure 2.4:Cables configurations

2.2.2 Lock in and lock out magnet

The process of locking magnet is related to life of magnet. First of all, one has to screw bolt out as also shown in Figure 2.5. But both of bolts should be screw in and tightly fixed, this is basically to prevent the free movement of magnet i.e. from moving on both sides out of control during a shipping process. For long journey of magnet, screw bolt in. This is necessary otherwise magnet move on either side i.e. left and right sides out of control and it may cause the shorter life time of magnet, and as a consequence of it magnet may be out of order or not operated well by some severe shockness. Use "RESET" button which is on front panel of main body system, this will favor to bring magnet to its initial position back and then magnet is ready to run with well set initial configurations.

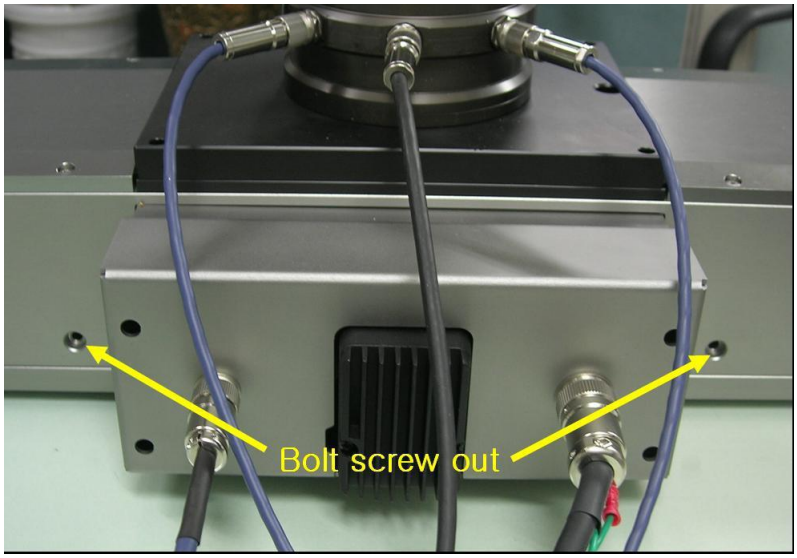

Figure 2.5: Screw bolt out of magnet

2.2.3 Liquid Nitrogen Tank and sample board Description

Description of liquid nitrogen tank and sample board is shown in Figure 2.6 and Figure 2.7.

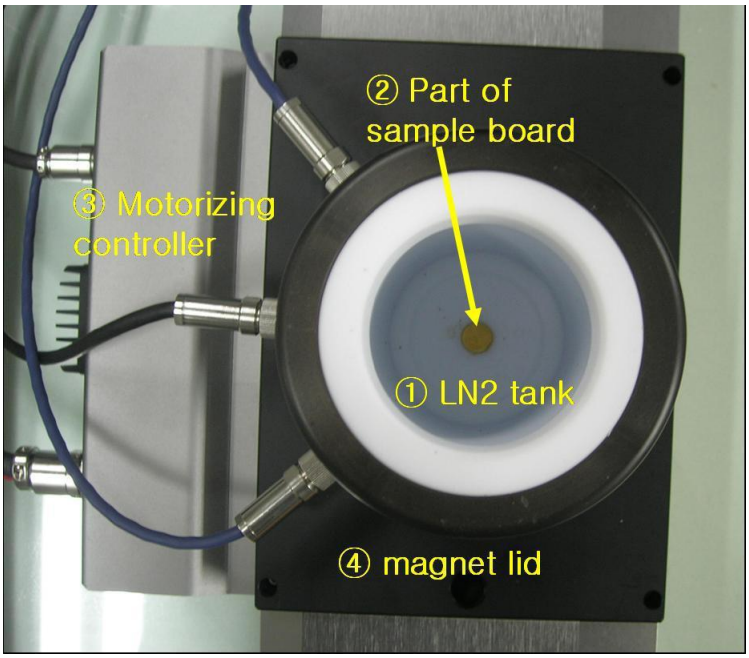

Figure 2.6: Liquid nitrogen tank

The Figure 2.6 also shows top view of liquid nitrogen tank and main features of its construction. One can view the part of sample board as well in Figure 2.6.

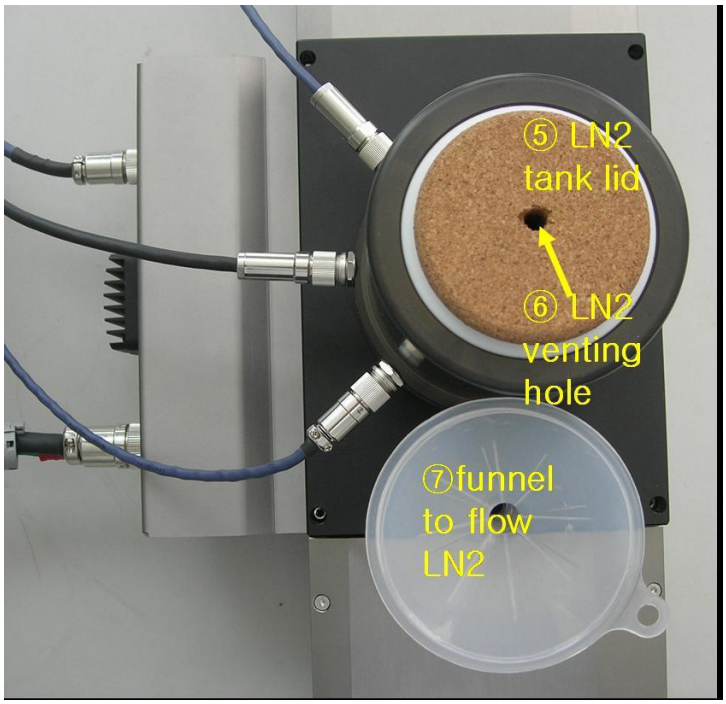

Figure 2.7: Lid of LN2 tank and funnel

The Figure 2.7 shows lid of liquid nitrogen tank and funnel which is used to flow LN2.

2.2.4 Functionalities for different parts at LN2 Tank and Sample Board

General portrayal of LN2 tank and magnet lid which is integrated with sample board as shown in Figure 2.8.These parts are not removable so there is not a single possibility to take it to pieces by means of force. Every part on this configuration has different functionality as functions of each part are as follows

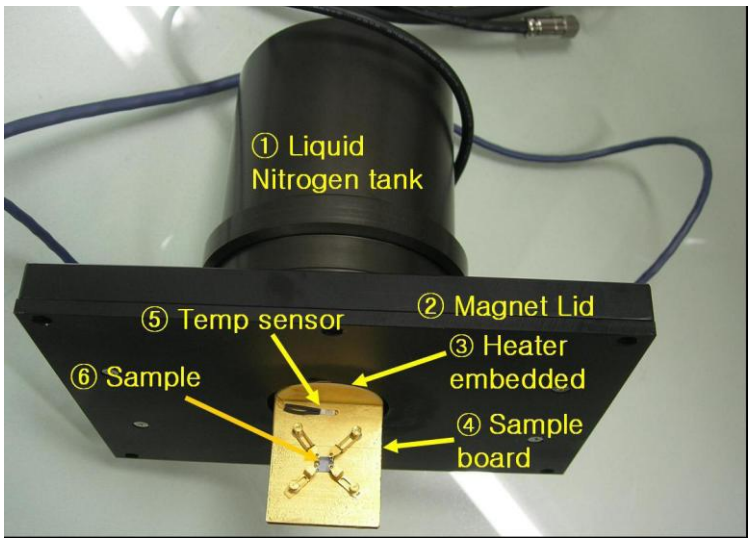

Figure 2.8: LN2 tank and magnetic lid with sample board

2.2.4.1 Task of LN2 tank

Liquid nitrogen is used to characterize thin samples at variable temperature range. LN2 must be poured into liquid nitrogen tank to test in variable temperature especially when one has to do electrical characterization at low temperature range.

2.2.4.2 Function of "part of sample board"

Part of sample board means the top end of sample board on which sample is mounted. Sample board has different feature in its construction like it is made of Oxygen free bronze and then it is coated by gold. Reason for using Oxygen-free bronze in construction of sample board is that oxygen free bronze is very sensitive to temperature variation and then the reason of gold coated sample board is that it can prevent sample board from getting more rusty.

2.2.4.3 Role of motorizing controller

Motorizing controller is used to move magnet on both sides either on left or right side during test of thin samples.

2.2.4.4 Role of LN2 tank lid

Lid of LN2 tank should be congested after pouring liquid nitrogen into LN2 tank. This lid is used to keep LN2 for longer span of time otherwise liquid nitrogen does boil from LN2 tank and as a result it evaporate with fast rate [1].

2.2.4.5 Job of Funnel

To flow liquid nitrogen into square type LN2 tank is done by use of funnel.

2.2.4.6 Function of Heater

Inside the sample board, heater is embedded. The function of embedded heater is to raise the temperature which goes up after getting some signals from electrical power.

2.2.4.7 How Sample board is heated and cooled

Sample board is heated by use of heater and if cooling purpose required then it is cool down by pouring of liquid nitrogen.

2.2.4.8 Function of Temperature Sensor

On the actual real time basis temperature sensor tells temperature, and then transfers this signal to system of main body.

2.2.4.9 Placement of Sample on sample board

On sample board, Sample should be mounted. It is important process for measurements. Un proper mounting of sample on sample board result to lose connection between tip of each probe and sample's four point edge especially in case when operate at low temperature.

2.3 Process of making Contacts on a thin Sample

This is most essential process for Hall measurements. Without making contacts properly on the sample, one cannot proceed for Hall measurements. Indium tin (InSn) compound [1] is used for making proper and good suitable contacts. Silver paste is also used for making contacts on a sample but contacts of Indium tin are preferred here.

2.3.1 Properties of proper contacts on Sample

The Van der Pauw method is 1 of most commonly used techniques for four-probe resistivity measurement. This gives an easy method to find out the sheet resistance of any semi conductor sample [2]. If the thickness of sample is known then one can calculate the resistance or conductance (inverse of resistance) of sample [3]. Essential condition for applying Van der Pauw method is that the thickness of sample should be much less in comparison with the length and width of the sample. For the best calculations of Hall measurements, it is favored that sample is symmetrical and sample contacts should be more proper on the sample. Properties of proper contacts on sample should include these features as

- Four contacts be placed on preferred sample geometry, these contacts must be ohmic.
- Infinite Small Contacts are preferred.
- Contacts must be as small as possible; i.e. error of any type given by their non-zero size must be order of D/L, where the average diameter of the contact is D and distance between the contacts is L.
- Same material must be used in making all contacts. This is to minimize or avoid the effects of thermoelectric.
- No temperature difference throughout the same sample otherwise it will cause contact errors.
- Contacts must place symmetrically on sample surface.
- Contacts on corners of sample are preferred rather than edges.
- Square type of sample geometry is preferred for proper placements of contacts.
- One of important feature is that within sample, there must be no isolated holes otherwise it will cause contacts errors.

2.3.2 Distinction between Ohmic Contacts and Blocking or Schottky Contacts

On a semi conductor device, an ohmic contact is a region that has been prepared so which shows the current-voltage curve of the device is symmetric and linear [4]. If asymmetric and non-linear current-voltage characteristic is obtained then the contacts are termed as a Schottky or blocking contacts [5]. Contacts of ohmic nature on semiconductors are evaporated or sputtered and in other words, using photolithography these are patterned. Stable contacts and low resistance are of critical importance for the reliability and performances of integrated circuits and even their preparation and different characterization are major and chief efforts in fabrication of circuits.

2.3.3 Methods of making contacts on samples

There are different methods for making contacts on a sample of either semi conductors or metals. The materials which can be used for making contacts include silver paste and Indium tin (InSn). Soldering contacts are made on four corners of square sample geometry. Methods adopted for making contacts are as follows [1]

1) Making soldering contacts on corners by using soldering iron.
2) Making contacts on corners by use of hand.

2.3.3.1 Making soldering contacts on corners by using soldering iron

Making soldering contacts on sample of thin films by making use of soldering iron is very important method. One of necessary condition for applying this method is that sample should be like that which is not affected by heated soldering iron. Sample board, cutting knife, tweezers, Temperature controlling soldering iron, indium tin (InSn) compound are required for this operation of making contacts as shown in Figure 2.9.

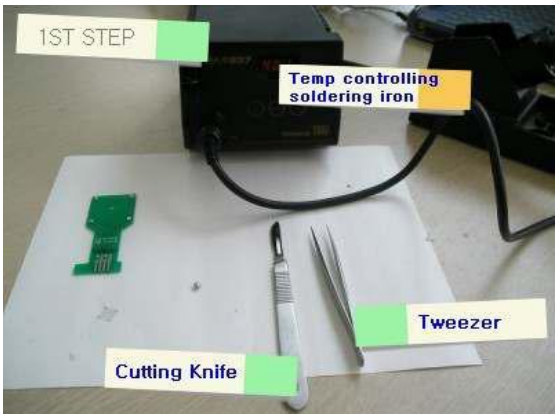

Figure 2.9: Apparatus require for soldering

First of all indium tin compound is melted, that is essential for soldering process. Set up soldering iron up to temperature i.e.350℃ ~ 400℃. Suitable temperature is required for melting Indium tin because very high temperature can cause indium tin to boil and very low temperature is not enough for Indium tin compound to melt. Visible description for temp controlling soldering iron is shown in Figure 2.10.

Figure 2.10: Temperature controlling soldering iron

At some useless glass, place the indium tin compound and then put the soldering iron onto Indium tin, this cause to melt indium tin compound. The melted Indium tin compound has form as shown in Figure 2.11.

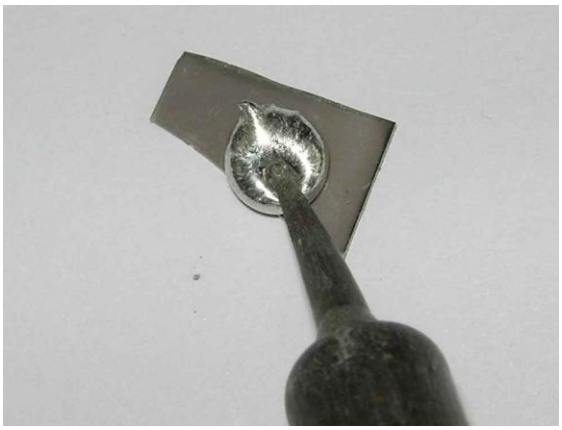

Figure 2.11: Melted Indium tin compound

At four point's edge of sample of square geometry, Soldering iron is used to perform soldering as shown in Figure 2.12. Annealing of one mint can be helpful if one has not annealed sample.

Figure 2.12: Soldering using iron

After soldering at four points edge, if soldered indium tin is not enough flat and has shape like mountain then through transparent paper Just slightly push on that soldered indium tin and this will cause Soldered point to adopt flat shape as also shown in Figure 2.13.

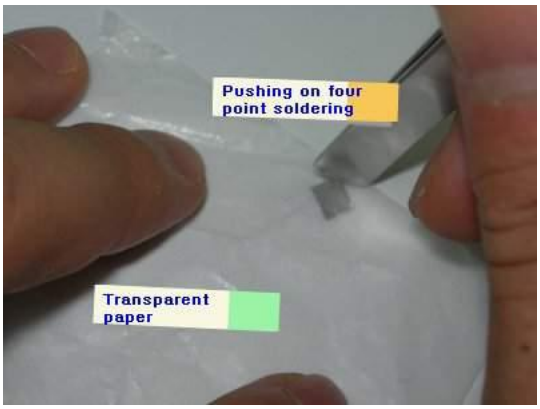

Figure 2.13: Making of flat soldered Indium tin contacts

Indium tin four points soldering is completed after various steps which described above. Final description after making contacts is as shown in Figure 2.14.

Figure 2.14: Sample after making contacts

2.3.3.2 Making contacts on corners by hand

This method is recommended if one has such sample of semiconductor which can damaged by applying heated soldering iron. With the help of knife, cut Indium tin compound into very small size as also shown in Figure 2.15. Indium tin is usually used because of decent properties of indium tin which relate to good electrical conductivity of this material. Carbon paste and Gold paste are also recommended to improve ohmic contacts for some samples.

Figure 2.15: Cutting of Indium tin compound

On corners of a sample after putting these small pieces of indium tin, through transparent paper just slightly and gently push up down as also shown in Figure 2.16. This will result in sticking indium tin on corners of semiconductor sample.

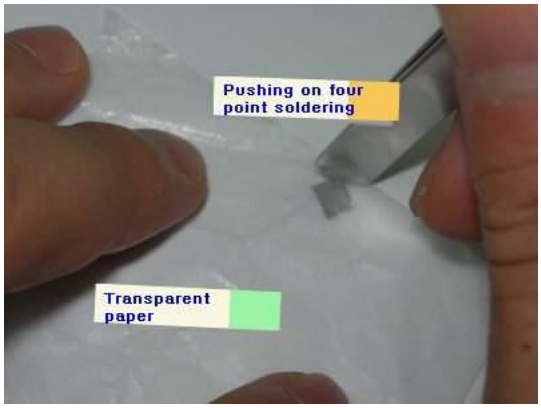

Figure 2.16: Sticking of Indium tin on corners of a square sample

Indium tin soldered four points after making contacts by hand is as shown in Figure 2.17.

Figure 2.17: Soldered four points by use of hands

2.4 Measurements in HMS-5000 System

After making complete software installation and successful suitable hardware connections, and then open measurement page. One can view that how to make measurements in range of variable temperature by selecting our temperature range in which one is willing to make measurements as also shown in Figure 2.18.

.

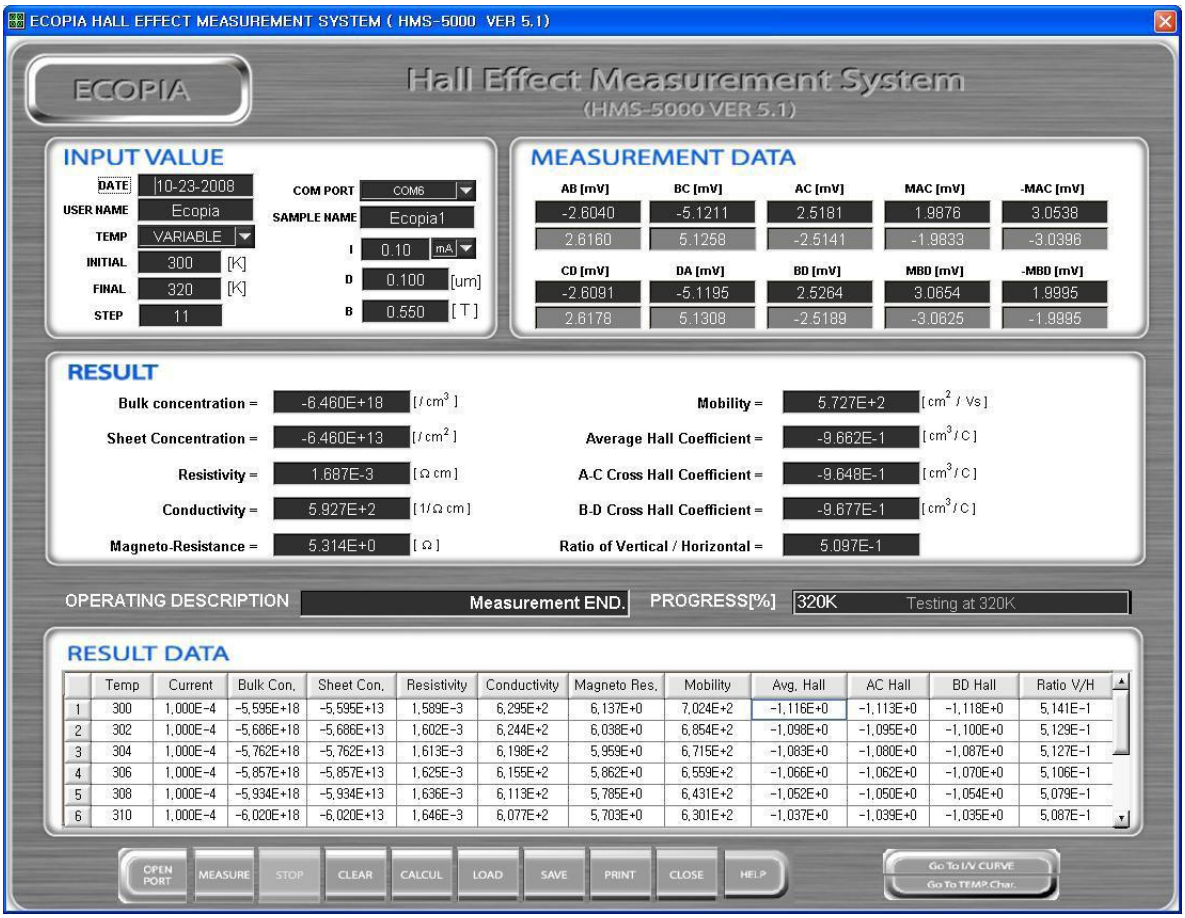

Figure 2.18: Main page of Ecopia 5000 Hall measurement system

Input values including temperature range, magnitude of current, magnetic field intensity and thickness of sample are given in chart of input values as also shown in Figure 2.19.

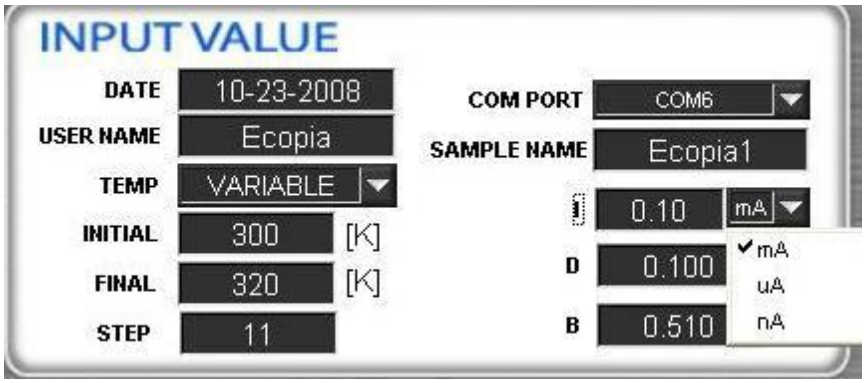

Figure 2.19: Chart for input values

In above chart of Input values, com port option should be filled either COM6 or COM1 depending upon the port which one is using. Temperature can be variable range or at room temperature. "I" means input value for current which ranges from 1nA to 20mA as require per sample's electrical properties. Lower value of current is preferred for highly resistive sample, if the sample is highly conductivity sample, then input current must be high enough i.e. 10mA or 15mA. "D" is thickness of sample; it can be measure by different methods. Here **"**B**"** is magneto flux density with magnitude of 0.55T. Magnet used in this apparatus can be little weaker or stronger which ranging from 0.53T to 0.57T. The reason behind is that permanent magnet is enough sensitive to air gap in between both magnets of round shape. **"**INITIAL**"** and **"**FINAL**"** mean variable temperature range in which one is willing to test. **"**STEP**"** stand for actual testing point. Check open port and if it gives connection success then one can do hall measurements. After complete measurements at the first step of temperature, system automatically raises temperature by means of heating up bronze sample board which favors to reach to temperature of next step. Similarly it is done for all steps of temperatures. Measured data are as shown in Figure 2.20.

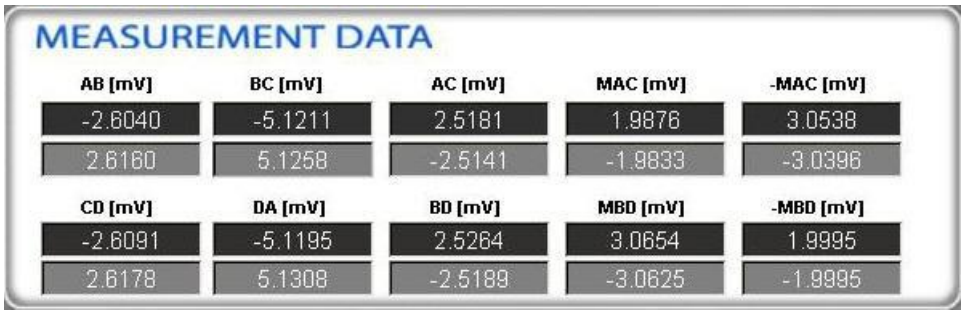

Figure 2.20: Measured data for quality of contacts

First black color row is for when system applied forward current and the second gray color row is for when system applied reverse current. One can estimate either our contacts are ohmic or non-ohmic by viewing each values like when forward and reverse currents are applied then values of voltages received are -2.6040and 2.6160 across contacts A and B, as these values are enough close so contacts are ohmic otherwise regard as non-ohmic contacts.

Sheet and bulk concentrations, resistivity, mobility, conductivity and magneto-Resistance are shown as results in Figure 2.21.

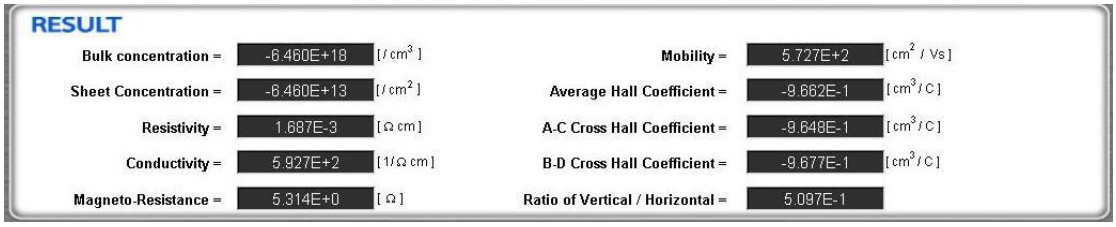

Figure 2.21: Measured results

One can explore data for IR and IV curve by giving temperature and current range. Temp Chart also gives us plots of resistivity, hall coefficient, carrier concentration, conductivity, mobility as a function of temperature.

2.5 Measurements at low temperature

Liquid Nitrogen is used for measurements at low temperature. Various steps are done for performing measurements at low temperature. These steps are as follows

1) First of all pour Liquid Nitrogen fully into liquid nitrogen tank of square shape as also shown in Figure 2.22.

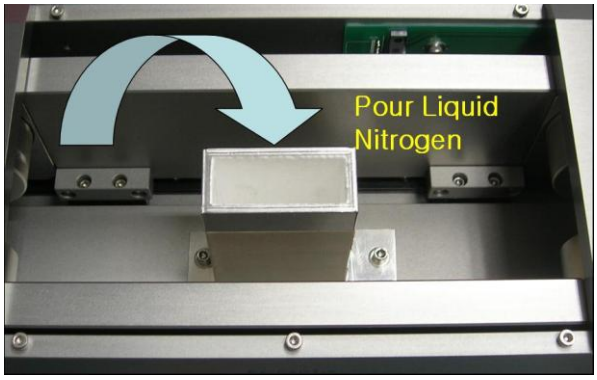

Figure 2.22: Pouring of LN2 into square LN2 tank

2) Second step is to close magnet lid which is integrated with sample board and liquid nitrogen tank.

3) Third step involved enough pouring of Liquid Nitrogen and then close LN2 tank lid as shown in Figure 2.23.

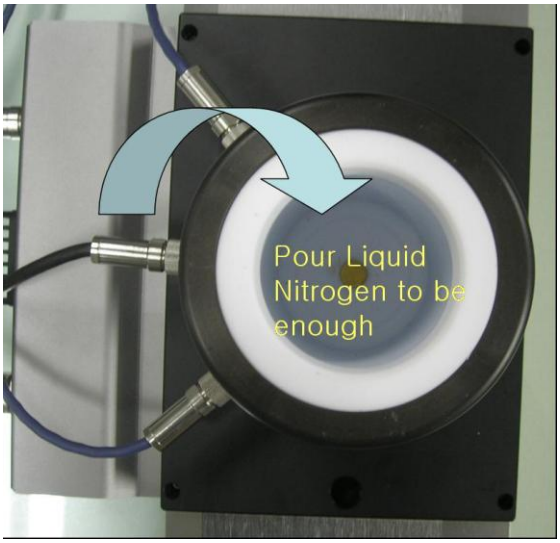

Figure 2.23: Pouring of LN2 into round shaped LN2 tank

4) Next step is to click **"**COM PORT**"**. If it shows "connection success" then the system is approaching currently temperature and if it indicates currently temperature in **"**Progress (%)**"**, then one can see step by step temperature goes down in **"**Progress (%)**"**.

5) Pouring of liquid nitrogen through funnel is the fifth step as also shown in Figure 2.24. Pouring of liquid nitrogen is necessary if one has to operate at quite low temperature.

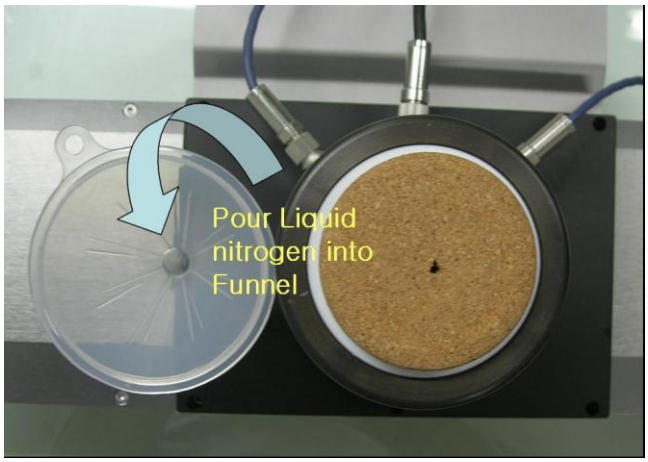

Figure 2.24: Pouring of LN2 through funnel

6) If desire operating temperature is achieved by above LN2 pouring process then go for measurements purposes. It favors to measure hall measurements of sample at variable temperature range especially when one is willing to operate at quite low temperature.

2.6 Some features related to Liquid Nitrogen and Sample Swapping

If liquid nitrogen is contacted with either clothes or skin then Liquid Nitrogen can prove dangerous [6] so pay extra attentions while performing with liquid nitrogen. Drying of sample and sample board is main procedure when one wishes to test different samples one another. Just after performing of experiment, one must never try to take out the sample board which is integrated with magnet lid from LN2 tank of square type. If one does that then it will cause both the sample board and sample be dewy if these are taking it out of liquid nitrogen tank. For the sake of convenience without taking out sample board with sample, just set up temperature 330K in initial and final and set up 3 steps and then do measure. This will cause the sample board along with sample be dried and then one can change the sample easily without facing any serious problems.

2.7 References

[1] www.bridgetec.com

[2] L. J. van der Pauw, Philips Research Reports ,vol. 13,pp.1,1958.

[3] L. J. van der Pauw, Philips Technical Review ,vol. 20,pp.220-224,1958.

[4] H.J. Moller, Semiconductors for Solar Cells, Artech, boston, pp.289,1993.

[5] B.G. Streetman, Solid State Electronics Devices, 4th ed. Prentice-Hall, Inc. 1995.

[6] www.chem.purdue.edu/chemsafety/chem/LN2

CHAPTER 3

3.0 Electrical Characterization of Zinc Oxide Thin films

Zinc oxide thin film belongs to group II–VI semiconductors with large value of excitation binding energy i.e. 60 meV and with direct band gap i.e. 3.37 eV [1], It is the only n-type semiconductor with zinc telluride from group II-VI semiconductors materials. ZnO thin films are of great significance for wide variety of applications such as gas sensors, organic light-emitting device (OLED) displays, transparent electrode for flat panel displays and solar cells, semiconductor diode lasers with characteristics of short wave length (SDLs) and for surface acoustic wave (SAW) devices and photoconductive UV detectors etc. [2-5]. The properties of ZnO can be tailored for spintronic applications through doping different transition metals ions, such as Co, Mn, V, Fe etc into the ZnO lattice [6-10]. ZnO thin films with characteristics of low resistive and highly transparent nature have been fabricated and synthesized using various deposition methods like sputtering [11], sol-gel method [12] and pulsed laser deposition [13]. Sol-gel method is preferred because of its uniform, simple, and very low cost ZnO thin films depositions [14]. This research reports the dc electrical resistivity measurements made on ZnO thin films received from thesis [15]. The dc electrical resistivity is ~ 10^3Ohm-cm at room temperature which agrees with the reported data [16]. Decreasing trend of resistivity and sheet resistance with increase of thickness of the films is also observed for ZnO thin film which verifies the semiconductor behavior. Magneto resistance variation with temperature is also reported for ZnO thin films. IV characterization of ZnO thin films under influence of light and dark conditions show that ZnO can be used as photovoltaic material.

3.1 Experimental procedure

One of our colleagues has prepared ZnO thin films at our School of Chemical and Materials Engineering (SCME), NUST and then I have characterized these thin films electrically as a function of temperature by Ecopia 5000 Hall Measurements System at

Thermal Transport Laboratory, SCME. Variable hopping model appears to be suitable to explain dc electrical resistivity of these thin films which favor semiconductor behavior. Morphological, structural and optical studies have done by [15]. So some of the results of SEM and XRD are mentioned here to indicate the morphology and crystal structure of ZnO thin films. ZnO thin films were prepared using Microscopy glass slides (Cat. No. 7105) as substrate for the sol-gel deposition of ZnO thin film. For the span of 10 minutes, Glass substrates were dipped in chromic, and then neutralized with the help of sodium hydroxide and then in the end rinsed in de-ionized water, rinsing in the end favored to remove contamination on the surface. For 10 minutes, the substrates were dried at 100°C in an oven after cleaning for details see the thesis [15]

These ZnO films were characterized by SEM, EDX, and XRD, the results are shown below. The magneto resistance and electrical resistivity measurements are done by Ecopia 5000 system as a function of temperature.

3.2 SEM analysis

Figure 3.1 shows morphology of ZnO thin films at low and high magnification with the help of SEM surface micrographs [15]. Irregular fiber-like streaks are observed at low magnification and if the coating thickness is increased, these irregular fibers like streaks become less and less dominant. Films are seen to be more homogeneous and formed by an agglomeration of submicronic particles at high magnification images. Grains coarsening took place by increasing the number of coating cycle and the grain size increased and found to be 54nm for 3 coating cycles and 92 nm for 10 coating cycles, which is in agreement with the crystallite size that is calculated from XRD analysis.

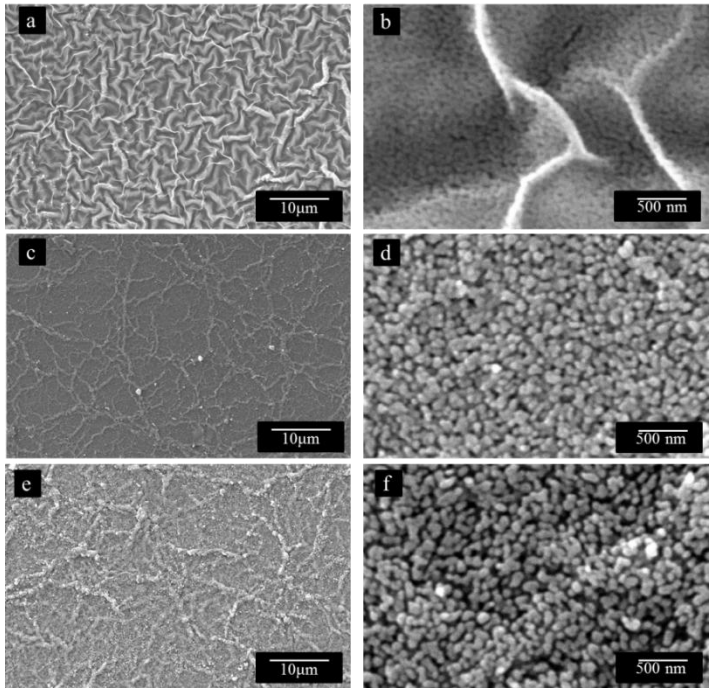

Figure 3.1: SEM micrographs of ZnO films for (a) 3 layers, (c) 5 layers, (e) 10 layers. (b), (d), and (f) are magnified SEM images of the three samples respectively with different thickness.

Mass percentage of deposited ZnO has confirmed by the EDS analysis. The mass percentage increases by increasing the coating cycles or thickness. Figure 3.2 shows the mass percent and the visual grain size of films as a function of the number of coating cycles. It is clear from the figure that the grain size increases almost linearly with the increase of layers and the mass percent of ZnO also increases.

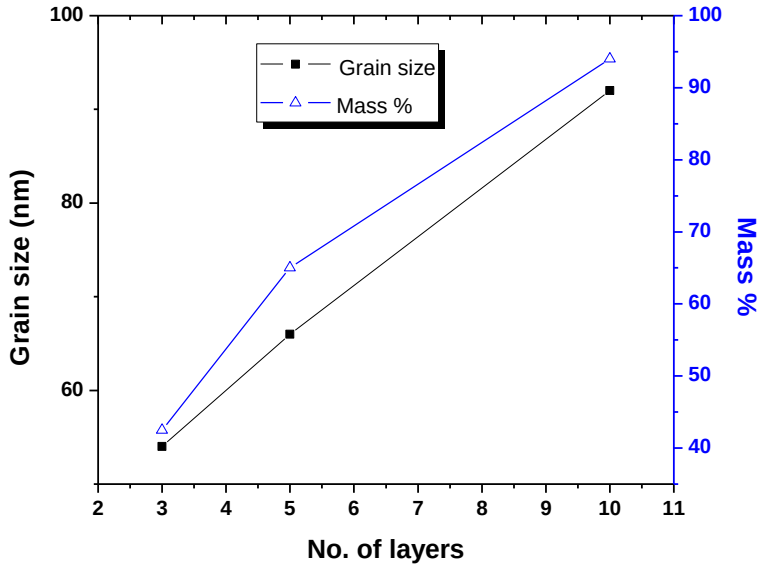

Figure 3.2: Mass percentage and grain size for 3, 5, and 10 layers.

3.3 Phase analysis and particle size

Figure 3.3 shows XRD patterns of ZnO thin films with different thickness annealed at 500°C [15]. Hexagonal wurtzite structures are found in all patterns. These all XRD peaks were identified and matched with the help of standard card JCPDS 36-1451in the recorded range of 2θ. Figure 3.3 shows XRD diffraction pattern of the deposited films with peaks matching with wurtzite ZnO (100), (002), (101), (102), and (110) faces. Because of thick nature of film, no preferential growth was observed. Using the Scherrer equation (3.1) Crystallite size (l) was also calculated as

$$l = \frac{0.94\lambda}{B\cos\theta} \qquad (3.1)$$

Whereλ is the X-ray wavelength which is used for analysis and has value as 1.5406 Å, θ is Bragg's angle of diffraction. And B is basically the broadening of diffraction line measured at full width at half maximum of its intensity.

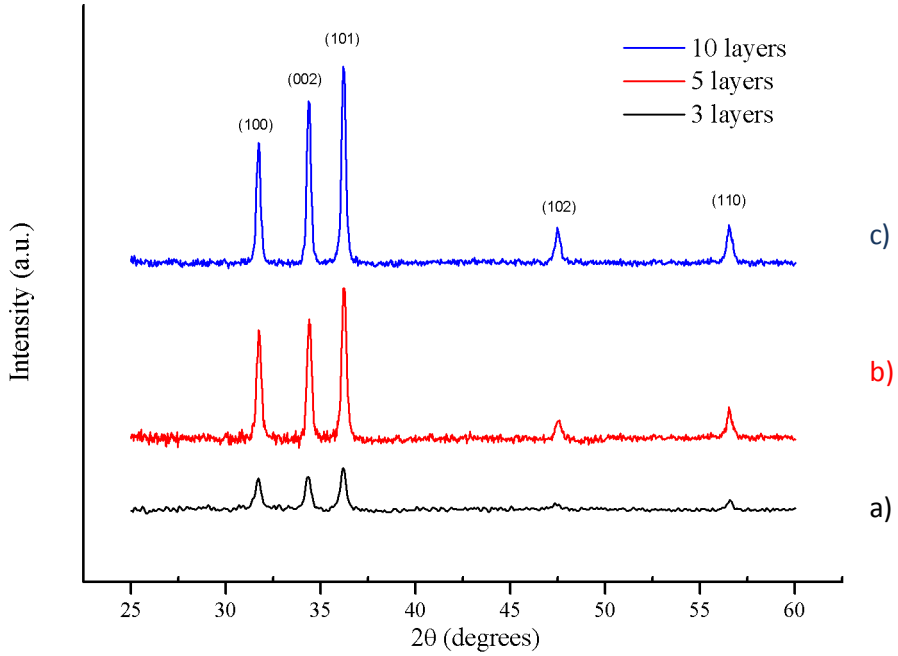

Figure 3.3: XRD pattern of ZnO films; (a) 3 coating cycles, (b) 5 coating cycles, (c) 10 coatings cycles.

The average crystallite size corresponding to (101) peak for three samples are shown in Table 3.1 along with the grain sizes. It is evident from the table that the crystallites as well as the grain sizes increase with the thickness of ZnO films. The crystallite size and grain size are given in Table 3.1 for different thicknesses [15].

Table 3.1Properties of ZnO films

Sample name	Thickness nm	Number of layers	Crystallite Size (XRD)(nm)	Grain Size (SEM)(nm)	Avg. crystallite size for (101) peak(nm)
a	860nm	3	31	54	28
b	1110nm	5	49	67	43
c	1510nm	10	64	92	58

3.4 Hall measurements

3.4.1 Sheet magneto resistance as a function of temperature

Indium tin was used for making contacts on samples of thin films for electrical measurements. Samples of ZnO thin films were with square geometry. Resistance of materials changes with applied magnetic field. Sheet magneto-resistance effect depends upon relative direction of applied magnetic field with respect to current and applied magnetic field itself. Sheet magneto resistance of ZnO thin films as a function of temperature with constant magnetic field 0.55 T are shown in Figure 3.4.

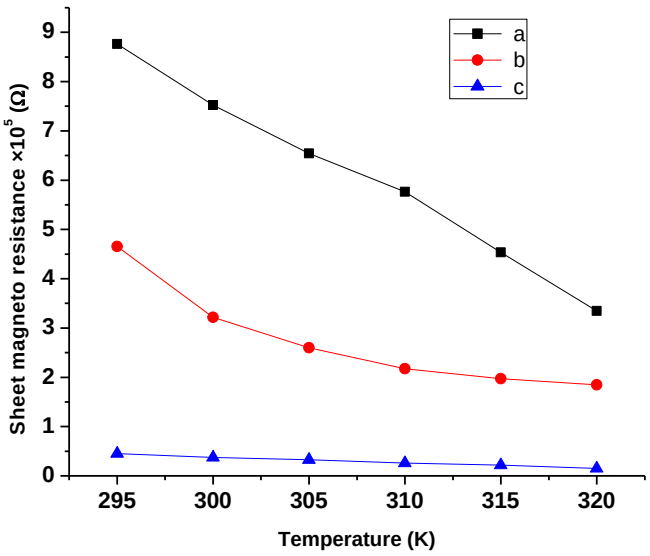

Figure 3.4: Sheet magneto resistance as a function of temperature with the constant magnetic field 0.55 T.

In this case, a magnetic field of low intensity of 0.55 Tesla was applied and current was taken as 0.1 micro Ampere depending upon the electrical properties of the sample. Magnetic field remained constant in this case. Temperature was ranging from 295K to 320K. Decreasing trend of magneto resistance with increasing temperature was observed for ZnO

thin films with different thicknesses. It was also observed that with increase of thickness, magneto resistance decreased. Higher values of magneto-resistance for different thickness have been found in ZnO thin films. As magneto resistance are found to be in order of 10^4 or 10^5 for these three thin films so change in resistivity for ZnO thin films are more than 2 % of order of change in resistivity which shows that ZnO is ferromagnetic material so it observe anisotropic magneto resistance phenomenon [17].

3.4.2 Resistivity and sheet resistance measurements with thickness

Resistivity measurements of ZnO thin films for different number of layers are done. Resistivity is calculated using Van der Pauw method. It is found that resistivity of ZnO thin films at room temperature is of order of 10^3Ohm-cm, which agrees with the previous reports [16]. It is also observed that in case of ZnO thin films, resistivity decreases with increase of the thickness of the films [18]. For samples a, b and c , resistivity observed was 6650 ohm-cm,5310 ohm-cm, 2560 ohm-cm respectively which also confirm that resistivity decreased with increase of thickness. Graphs for resistivity and sheet resistance as a function of thickness are also shown in Figure 3.5.

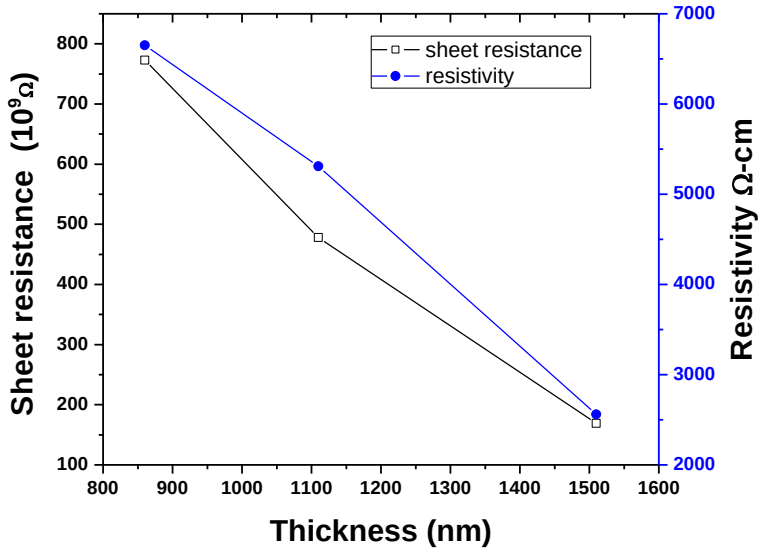

Figure 3.5: Sheet resistance and dc electrical resistivity of ZnO as a function of the thickness

As resistivity has direct relation with sheet resistance (R_s).

R_s× thickness= Resistivity (3.2)

So sheet resistance also decreased with increase of thickness or cycle coatings. For samples a, b and c, sheet resistance were found to be 773,478 and 169 giga ohms respectively.

3.4.3 Hall coefficient of ZnO thin films

As Hall coefficients for these three thin films were measured via Ecopia 5000 Hall Effect Measurements System and these are all found to be negative which indicate that ZnO thin films are of n-type with more concentration of electrons as charge carriers. Our observations agree with the earlier reports [19]

3.4.4 Mobility and concentration as a function of No. of layers

Bulk concentration and mobility have been found with help of Ecopia 5000 Hall Measurement System. Figure 3.6 shows that bulk concentration (cm^{-3}) and mobility (cm^2/V_s) as a function of number of layers.

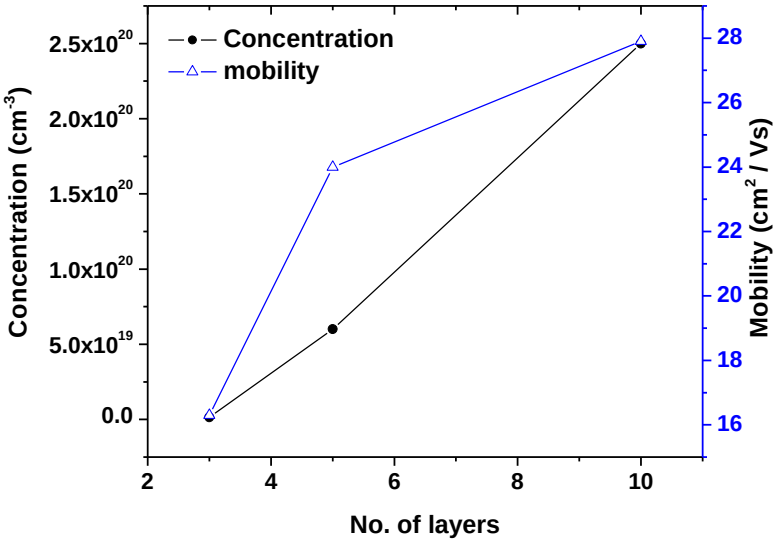

Figure 3.6: Concentration and mobility as a function of No. of layers

Bulk concentrations for three films of ZnO with number of layers i.e. 3, 5, and 10 are found to be 1.5E18, 6E19, 2.5E20 cm^{-3} which is in agreement with the report [20]. The mobilities of these three thin films are found to be 16.3, 24 and 27.9 cm^2/V_S which are again in agreement with [20]. It shows that with the increase of the number of layers mobility of carriers improved.

3.4.5 IV characterization of ZnO thin films

The IV characterizations of ZnO thin films under dark and under the influence of UV light at room temperature are shown in Figure 3.7 and Figure 3.8.

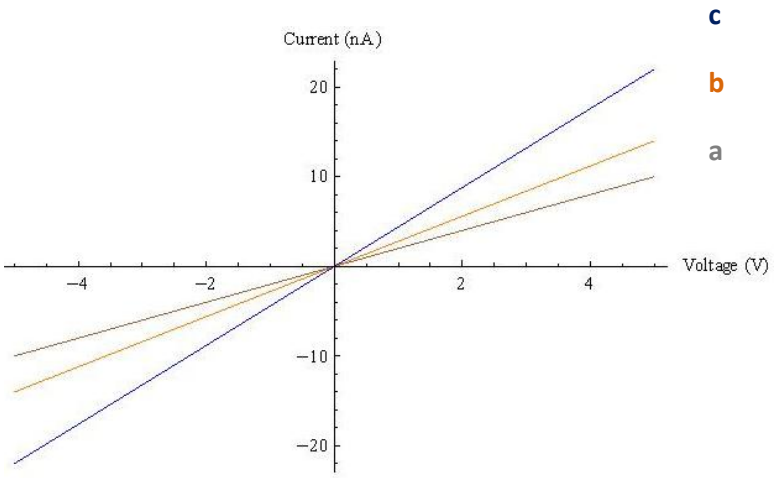

Figure 3.7: IV curves of ZnO thin films under dark condition

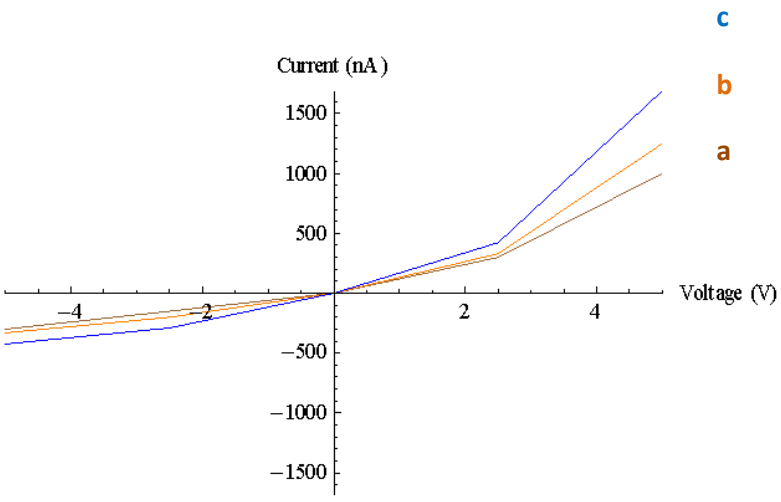

Figure 3.8: IV curves of ZnO thin films under UV light condition

ZnO thin film can be used in optoelectronics and sensors applications. Sol gel spin coated ZnO thin films are sensitive to UV-light and it is observed because of such electrical properties it can also be used as window material in photovoltaic applications. The I-V characteristics for dark and under UV-illumination have different features. The I-V characteristics for ZnO thin films with different thickness's under dark and UV-illumination are shown in Figure 3.7 and Figure 3.8. Dark condition is created by putting sample board on which sample is mounted under the tank of hall apparatus. Ohmic behavior in dark conditions for ZnO thin films is observed [21]. In the case of UV-illumination, as there is an increase of the production of electron-hole pairs so as a result of this, non-ohmic behavior is observed [21]. For ZnO thin films under dark and UV-illumination, the current at a given voltage is lower in case of dark conditions while in case of UV-illumination it is higher because of the higher production of electron-hole pairs. As light shows non-ohmic behavior in ZnO thin films so this feature can also be used as a photovoltaic material.

3.4.6 VRH Modeling on Zinc Oxide thin film

The dependence of electrical conductivity upon temperature is shown in Figure 3.9 for all of these three samples. The obtained semiconductor like behavior of electrical conductivity [22] is expressed by the relation

$$\sigma_{dc} = \sigma_0 \exp(-\Delta E / k_B T) \qquad (3.3)$$

Where σ_0 is the pre-exponential factor, ΔE is activation energy and k_B is the Boltzmann constant .Using equation (3.3), activation energy of the sample can be calculated from the slope of $\ln \sigma$ vs $1/k_B T$ plot. Obtained activation energies are 0.03 ± 0.01 eV for 860nm, 0.157 ± 0.004 eV for 1110nm, 0.173 ± 0.007 eV for 1510nm respectively with fitting coefficient of 0.99 in all of these cases.

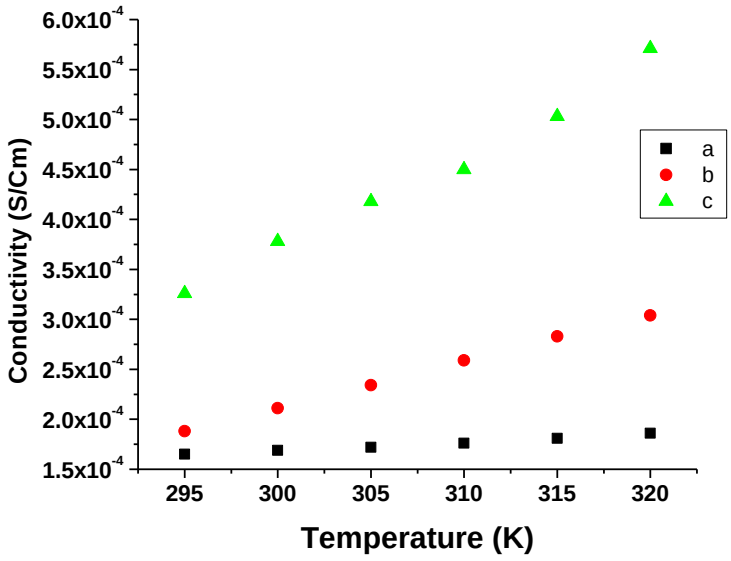

Figure 3.9: Variation of electrical conductivity with temperature

The value of pre-exponential factor σ_0 provides an identification of the fact that whether the conduction is due to extended states or is by localized states [23]. In order to conduct by extended state conduction, $\sigma_0$must be in the range of 10^3-10^4 S/cm [24] and there should be a smaller value for the hopping conduction between localized states, in which electrons hop between one localized states to the next separated by the energy gap. In all of these three samples, the value of σ_0 lies between 10^{-4}- 10^{-1} S/cm. These values confirm that the conduction takes place by the hopping mechanism. Small values of activation energy for these three thicknesses provide further confirmation of the hopping phenomenon [25].

In order to fulfill some necessary conditions, it is assumed that hopping process is governed by Mott's Variable Range Hopping (VRH) mechanism expressed as [26, 27]:

$$\sigma = \sigma_o \exp\{-(T_o/T)^{1/4}\} \qquad (3.4)$$

Where T_o is the degree of disorder expressed by $T_o = \lambda\alpha^3/\{k_B N(E_F)\}$, and $N(E_F)$ is the density of states at fermi level, λ is dimensionless constant of about 16 [27, 28] and α represents localization length of excited electron ($10^7 cm^{-1}$). Mott VRH plot for these three samples are shown in Figure 3.10. The hopping distance (R) and average hopping energy (W) are calculated by the following relations as a function of temperature [27], and are shown in Table 3.2.

$$R = \{9/(8\pi\alpha k_B T N(E_F))\}^{0.25} \quad (3.5)$$

$$W_{dc} = 3/(4\pi R^3 N(E_F)) \quad (3.6)$$

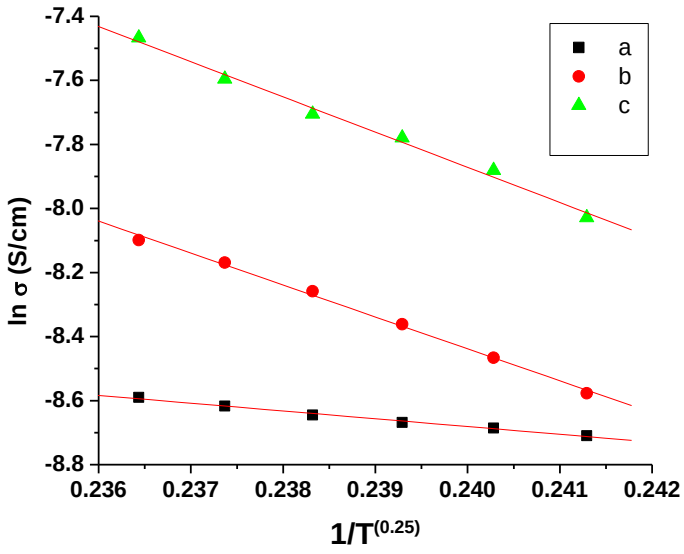

Figure 3.10: Mott's VRH plots for (a) 860 nm (b) 1110 nm and (c) 1510 nm samples

It is clear from Table 3.2 the hopping distance decreases while hopping energy increases linearly with rising temperature. The necessary conditions for applying Mott's VRH mechanism are [25]

(i) average hopping energy must be greater than thermal energy (i.e. $W_{dc} > k_B T$) *and*

(ii) $\alpha R > 1$

Here both the conditions are satisfied in all of these three samples.

Table 3.2: **Hopping Energy and Hopping distance for three ZnO thin films**

Temp	Sample a		Sample b		Sample c	
(K)	R (nm)	W (meV)	R (nm)	W (meV)	R (nm)	W (meV)
295	2.25E+00	3.82E+01	9.29E+00	1.57E+02	1.02E+01	1.72E+02
300	2.24E+00	3.86E+01	9.25E+00	1.59E+02	1.01E+01	1.74E+02
305	2.24E+00	3.91E+01	9.21E+00	1.61E+02	1.01E+01	1.76E+02
310	2.23E+00	3.96E+01	9.17E+00	1.63E+02	1.00E+01	1.78E+02
315	2.22E+00	4.01E+01	9.14E+00	1.65E+02	9.99E+00	1.81E+02
320	2.21E+00	4.06E+01	9.10E+00	1.67E+02	9.95E+00	1.83E+02

So for the samples namely a, b, c $N(E_F)$ is 5.47E+20,1.9E+18 and 1.33E+18 respectively and R(nm) is 2.25±0.02, 9.29±0.20, 10.0±0.50 respectively while W_{dc} is 38.2 meV,157meV and172meV respectively.

3.5 Summary

ZnO thin films are prepared by sol gel method. These films are characterized by SEM, XRD, EDS and Hall Effect Measurement system for their morphological, structural, and electrical properties. Crystallite size and grain size determined by XRD and SEM. Electrical resistivity of ZnO thin film are found to be of the order of 10^3 ohm-cm. Decreasing trend for magneto resistance with temperature is observed, ZnO thin films observe anisotropic magneto resistance phenomenon. Resistivity and sheet resistance variations with thickness are also determined. IV characterizations for films under UV light and dark conditions

showed features which is responsible for its applications in photovoltaic materials. The resistivity of ZnO thin films also follows the hopping model.

3.6 References

[1] H.Benelmadjat, B.Boudine, O.Halimi, M.Sebais: Optics & Laser Technology 41(2009)630–633.

[2] L.Znaidi, Sol–gel-deposited ZnO thin films: A review, Materials Science and Engineering B 174 (2010) 18–30.

[3] S. O'Brien, L.H.K. Koh, G. M. Crean, ZnO thin films prepared by a single step sol–gel process, Thin Solid Films 516 (2008) 1391–1395.

[4] D. Basak[a],*, G. Amin[b], B. Mallik[b], G.K. Paul[c], S.K. Sen[c]: Journal of Crystal Growth 256 (2003) 73–77.

[5] Chien-YieTsay, Kai-Shiung Fan, Yu-Wu Wang, Chi-Jung Chang,Yung-Kuan Tseng, Chung-Kwei Lin, Transparent semiconductor zinc oxide thin films deposited on glass substrates by sol–gel process, Ceramics International 36 (2010) 1791–1795.

[6] S. Deka, P.A. Joy: Solid State Commun. 142(2007) 190.

[7] A. Debernardi, M. Fanciulli, Physica B 401-402(2007)451.

[8] A. J. Chen, .X. M. Wu, Z. D. Sha , L.J Zhug, Y. D. Meng : J.phys. D.Appli. Phys. 39(2006)4762.

[9] M. Naeem, S.K.Hasanain, A.Mumtaz : J.Phys: Condens. Matter 20(2008)025210.

[10] M. Naeem, S.Qaseem, I.H.Gul, A.Maqsood: J.Appl. Phys. 107(2010)124303.

[11] Tadatsugu Minami, Takashi Yamamoto, Toshiihiro Miyata: Thin Solid Films, Volume 366, Issues 1-2, 1 May 2000, p 63-68.

[12] M.N.Kamalasanan, Subhas Chandra: Thin Solid Films 288(1996) 112-115.

[13] B.L.Zhu,X.Z/Zhao,F.H.Su,G.H.Li,X.G.Wu,J.Wu,R.Wu : Vacuum, volume 84, issue 11, 4 June 2010, p 1280-1286.

[14] L. Znaidia, G.J.A.A. SolerIllia, S. Benyahia, C. Sanchez, A.V. Kanaev, Oriented ZnO thin films synthesis by sol–gel process for laser application, Thin Solid Films 428 (2003).

[15] S.Slam, Sol-Gel synthesis of transparent conductive oxide films for thin films based solar cells, MS thesis, Nust, 2011.

[16] T. Schuler, M.A. Aegret, Optical, electrical and structural properties of sol gel ZnO: Al coatings, Thin Solid Films 351 (1999) 125-131

[17] Magneto Resistance Overview: Janice Nickel, Computer Peripherals Laboratory HPL-95-60, June, 1995.

[18] Yung-KuanTseng ,Guo-JhanGao , Shih-Chun Chien: Thin Solid Films vol 518 (2010) 6259-6263.

[19] Y. Natsume, H. Sakata: Materials Chemistry and Physics 78 (2002) 170–176.

[20] Keh-moh Lin*, Paijay Tsai[1]: Thin Solid Films 515 (2007) 8601–8604.

[21] S.Ilican, Y.Caglar, M. Caglar: Journal of Optoelectronics and Advanced Materials Vol. 10, No.10, October 2008, p. 2578-2583.

[22] I.H. Gul, A.Z. Abbasi, F.Amin, M. Anis-ur-Rehman, A. Maqsood, J. Magn.Magn.Mater.311 (2007) 494.

[23] M. Fadel, A.A. Nigim, H.T Elshair, Vacuum 46 (1995) 1279.

[24] A.A. Dakhel, Cryst. Res. Technol. 41 (2006) 800-802.

[25] N.F. Mott, Philos. Mag. 22 (1970) 7.

[26] N.F. Mott, E.A. Davis, Philos. Mag. 22 (1970) 903.

[27] N.F. Mott, E.A. Davis, Electronic processes in nano crystalline materials, Clarendon, Oxford, 1979.

[28] A. Ganguly, S.K. Mandal, S. Chaudhary, A.K. Pal, J. Appl. Phys. 90 (2001) 5652).

CHAPTER 4

4.0 Electrical Characterization of Cadmium Sulfide Thin films

CdS belongs to II–VI group semi conductor with direct band gap i.e. 2.42 eV and n-type material [1]. Thin films of CdS have been used in variety of applications such as optical detectors, solar cells and in optoelectronic applications [2-4]. Because of its good optical and electrical properties, it has been used widely in many photovoltaic applications [5-8]. CdS has significant features due to its stability, low cost, high absorption coefficient and band gap [9].Two crystalline forms of CdS exist; these forms include hexagonal (wurtzite) phase and cubic (zincblende) phase. One can grow CdS thin films of both type of these phases. Deposition technique plays an important role for the development of either cubic or hexagonal phase [10]. For photovoltaic devices and high efficiency CdTe, as window material CdS thin films are being used widely [11]. For CdTe/CdS thin films solar cells, about 16% efficiencies have been reported [12]. High electrical resistivity has been found in un-doped CdS thin films but different dopants are used to decrease the electrical resistivity of CdS films. CdS thin films have been fabricated and synthesized using various deposition methods like chemical vapour deposition, spray pyrolysis , close space sublimation, thermal evaporation, vacuum evaporation, chemical bath deposition, sputtering, photochemical deposition, pulsed laser deposition and vapour transport deposition [13-20].This research reports the dc electrical resistivity measurements made on CdS thin films received from [21]. The dc electrical resistivity for CdS thin film is ~ 10^5Ohm-cm at room temperature. Decreasing trend of resistivity and sheet resistance with increase of thickness of the CdS thin films are also observed which verify the semiconductor behavior. Magneto resistance variation with temperature is also reported for different thickness of CdS thin films. The dc electrical resistivity for CdS thin films also follows the hoping model.

4.1 Experimental procedure

One of our Colleagues has prepared CdS thin films at our School of Chemical and Materials Engineering (SCME), NUST and then I have characterized these CdS thin films electrically as a function of temperature by Ecopia 5000 Hall Measurements System at Thermal Transport Laboratory, SCME. To explain the dc electrical resistivity of these CdS thin films which favor semiconductor behavior, variable hopping model appears to be suitable. Structural, morphological and optical studies have done by thesis [21]. Some of the result of XRD and SEM are mentioned here to indicate the crystal structure and morphology of these CdS thin films. CdS Thin films have many optoelectronics applications because of favorable optical and electrical properties of CdS thin films and using different methods, these films can be fabricated. Thermally evaporation technique is suitable for fabrication of CdS thin films which have been used for wide variety of applications [22-24]. Because of simple apparatus and high transport efficiency, fabrication of thin films using close spaced sublimation method has encouraging and suitable results [25]. These suitable results include well defined preferential orientation, high absorption coefficient and larger grain size which required for solar cells applications. Using close space sublimation method, on glass substrates these CdS thin films were deposited. Using pure IPA bath for 30 minutes, the substrates with dimensions of 25 mm x 75 mm were cleaned up. For fabrication of thin films, CdS powder (99.99% pure) of Aldrich (USA) was used as source material each time for the more details see the thesis [21]. Thickness of sample depends upon the deposition time i.e.

Table 4.1:Thickness Vs deposition time

Sample name	Deposition time(min)	Thickness nm
a	5	248nm
b	10	444nm
c	18	860nm

SEM and XRD were used to characterize CdS thin films, the results are shown below. The magneto resistance and electrical resistivity measurements are done by Ecopia 5000 system as a function of temperature.

4.2 SEM Analysis

Figures 4.1 show the morphology of CdS thin films at low and high magnifications with the help of SEM surface micrographs [21].

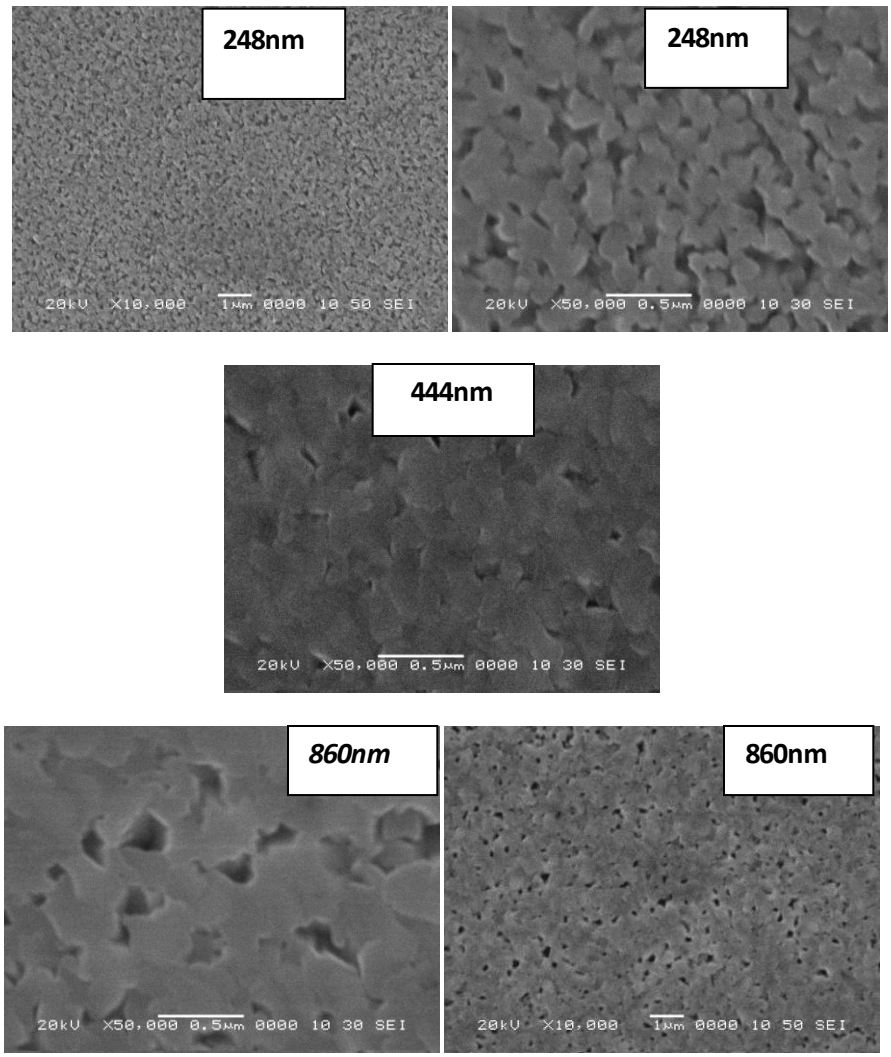

Figure 4.1: SEM graph of CdS sample a, b and c with thickness 248nm, 444nm and 860 nm respectively

With the help of SEM graphs, average grain sizes of the CdS thin films are calculated. For different samples, the values of grain sizes are different, which are shown in Table 4.2. But more or less, all grains are of similar sizes in each sample. It can be seen clearly that some voids/ pores (closed) are distributed in all the samples. In between different oriented grains, voids were filled during process of annealing and then this phenomenon could be supported and continued further if annealing time would have increased.

Table 4.2:Variation of grain size and grain density with Film Thickness.

Sample Name	Thickness (nm)	Average Grain Size (nm)	Dislocation density lines/m^2 (δ)	Grain Density (grains/m^2)
a	248	195.7	26.1×10^{12}	15.2×10^{12}
b	444	306.9	10.6×10^{12}	7.01×10^{12}
c	860	409.5	5.9×10^{12}	3.5×10^{12}

Table 4.2 shows that average grain size is increased with increase of film thickness and grain density is decreased with the increase of film thickness [26]. It also shows that as thickness of films increases, thin film grows in better manner with less stresses and defects as a result of it one can has larger grains. The dislocation density (δ) is defined as the length of dislocation lines per unit area, and has been projected using the following equation 4.1 [27]

$$\delta = 1/D^2 \qquad (4.1)$$

Where (δ) stands for measure of amount of defects in a crystal and D stands for size of grain. Good crystalline nature of CdS thin films are related to small amount of defects. For these CdS thin films, it was observed that in all samples, all grains are approximately of same sizes.

Mass percentage of deposited CdS has confirmed by EDS analysis. When CdS is sublimated then at higher value of temperature CdS compound dissociates into the S and Cd.

As depending upon different factors, for different samples different ratio of Cd and S is observed. 144.4 is the atomic weight of CdS compound, so starting composition of CdS powder is as

S = 32.066/ 144.46 = 0.222 = 22.2%

Cd = 112.4/144.466 = 0.778 = 77.8%

According to EDS data, end composition after deposition is as shown in Table 4.3 [21]

Table 4.3: CdS end composition after deposition

Sample	**Composition (Cd/S)**	**$Cd_{(1\pm x)}S_{(1\pm x)}$**
a	75.74/24.25	$Cd_{(0.98)}S_{(1.02)}$
b	78.87/21.13	$Cd_{(1.01)}S_{(0.99)}$
c	77.04/22.96	$Cd_{(0.99)}S_{(1.01)}$

Table 4.3 shows that end composition changed slightly in comparison with the initial composition.

4.3 Phase analysis and particle size

Using X-ray diffraction (XRD) technique figure 4.2 shows the XRD patterns of the CdS thin films with different thickness which prepared by close space sublimation process [21]. At 2θ scanning mode which ranging from 20 to 60 degree diffraction angle, the diffraction spectra was measured.

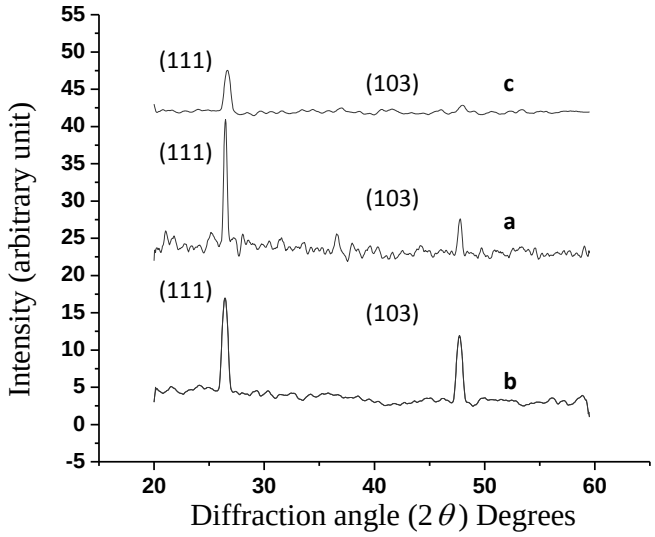

:

Figure 4.2: XRD patterns of the samples a, b and c

Depending upon conditions which used during growth of films, either hexagonal (Wurtzite) or cubic (Zinc blende) crystal structure for CdS films are reported [28]. Indication of polycrystalline nature of thin films just because of appearance of many peaks. The major peaks in case of all samples appear around 2θ of 26.547° and of 47.794°. With ASTM card numbers C01-080-0019 and C00-041-1049, the XRD pattern were matched, for peaks which appeared around 2θ of 26.547° and of 47.794° respectively. The main reflections for peaks are same, in which (103) plane represents hexagonal phase and (111) plane represents the cubic phase in growth of thin films. For different samples, intensities of reflection which corresponds to (103) plane are different. Strong reflection in all samples a, b and c, the crystallites which corresponds to the (111) plane of CdS of cubic structure satisfy condition i.e. a = b = c = 5.82 Å [29]. Using angular position of (111) diffraction peak and Bragg law, the lattice constant for these three samples were calculated. Average crystallite size 'd' of polycrystalline films is determined by applying the Scherrer formula

$$d(\text{Å}) = k\lambda(\text{Å})/(D\cos\theta) \qquad (4.2)$$

where k is the scherrer constant and it is taken as 0.9 [30], full width at half maximum in radians is represented by D and θ stands for Bragg angle in degrees which corresponds to the

maximum intensity of peak. For samples a, c, and b, crystallites size were found to be 199nm, 160nm and 140.7nm respectively. The crystallite size depends upon a lot of factors such as on the deposition rate, substrate temperature, annealing temperature and film thickness [31]. For samples a, c and b, lattice constants were found to be 5.831 Å, 5.8 Å and 5.838Å respectively, which agrees with the reported value i.e. 5.82 Å [29].

4.4 Hall measurements

4.4.1 Hall coefficient of CdS thin films

Hall coefficients for these three as deposited CdS thin films were found with the help of Ecopia 5000 Hall Effect Measurements System and these all hall coefficients are found to be negative which indicate that CdS thin films are of n-type [1] which shows these films are with more concentration of electrons rather than holes as charge carriers. These n-type films can be converted into p-type films with help of doping of Ag. Our observations agree with the earlier reported data [32].

4.4.2 Mobility and bulk concentration as a function of deposition time for CdS thin films

With the help of Ecopia 5000 Hall measurements system, mobility and bulk concentration have been measured for CdS thin films using indium tin contacts. Figure 4.3 shows that bulk concentration (cm^{-3}) and mobility (cm^2/V_s) as a function of deposition time. With increase of deposition time, thickness of the CdS thin films also increased.

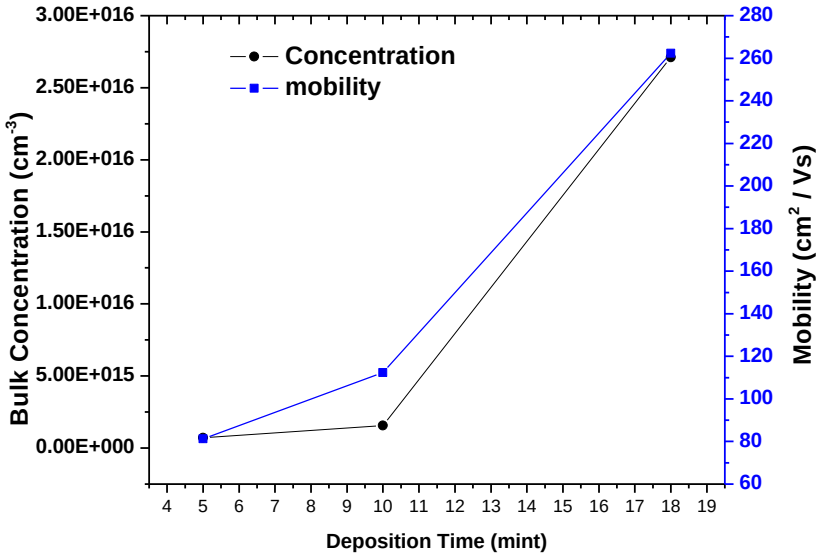

Figure 4.3: Bulk concentration and mobility as a function of deposition time for CdS thin films

Mobility for three CdS thin films with deposition time 5, 10 and 18 mints are found to be 81.3, 112.3 and 262.3 cm^2/V_S and similarly bulk concentrations for same deposition time are found to be 7.11E14, 1.56E15 and 2.17E16 cm^{-3} which is in agreement with previous reported data [33]. As the deposition time for films increased which corresponds to increase in thickness of CdS films and in the end mobility is being increased with increase in thickness or deposition time. As mobility and conductivity has direct relations and conductivity has inverse relation with the resistivity so with increase of deposition time, resistivity decrease which results with an increase of mobility of carriers.

4.4.3 Resistivity and sheet resistance measurements with deposition time for CdS films

Using Ecopia 5000 system, resistivity measurements of CdS thin films with different deposition time have been done. With help of Van der Pauw technique, resistivity is measured. At room temperature for CdS thin films, resistivity is found to be the order of 10^5 Ohm-cm, which has good agreement with the previous reported data [34]. As for

semiconductors thin films like ZnO and CdS thin films, with increase of thickness, resistivity decrease. Resistivity observed for different deposition time i.e. 5, 10 and 18 mints are 3.23E5 , 2.47E5 ohm-cm and 1.98E5 ohm-cm respectively at room temperature. Plot of sheet resistance and resistivity as a function of deposition time is shown in Figure 4.4.

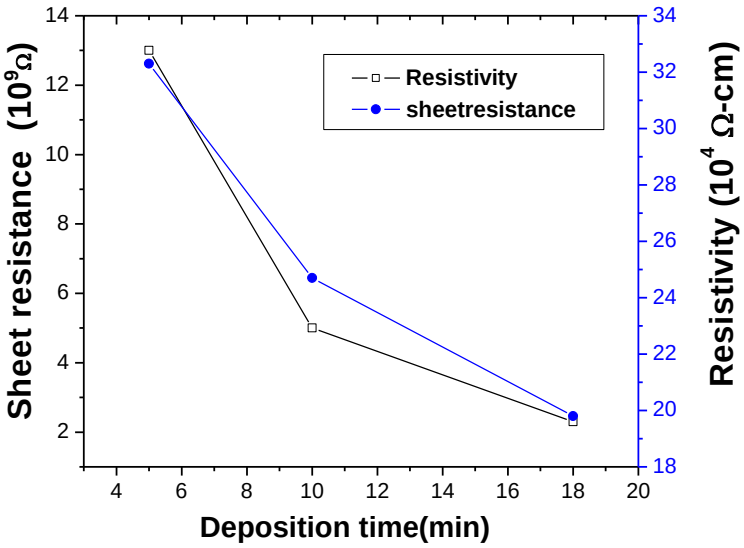

Figure 4.4: Resistivity and sheet resistance for CdS thin films as a function of the deposition time

As resistivity has direct relation with sheet resistance (R_s) so with increase of deposition time which corresponds to an increase of thickness, sheet resistance is found to be decreased. Sheet resistance values are found to be 13, 5 and 2.3 Giga ohms respectively for deposition times i.e. 5, 10 and 18 mints.

4.4.4 Sheet magneto resistance as a function of temperature for CdS thin films

Using Ecopia 5000 system, magneto resistance has been determined for CdS thin films with different deposition time. Contacts of Indium tin was made on CdS thin films for four

probe electrical characterization. Samples of CdS thin films were with square geometry. Effect of sheet magneto resistance appeared when CdS thin films were subjected to a magnetic field which resulted in a change of resistivity of CdS thin films. Sheet magneto-resistance effect depends upon relative direction of applied magnetic field with respect to current and applied magnetic field itself. With subject of constant magnetic field of strength 0.55T, sheet magneto resistance for CdS thin films with different deposition time i.e. 5, 10 and 18 mints as a function of temperature are shown in Figure 4.5.

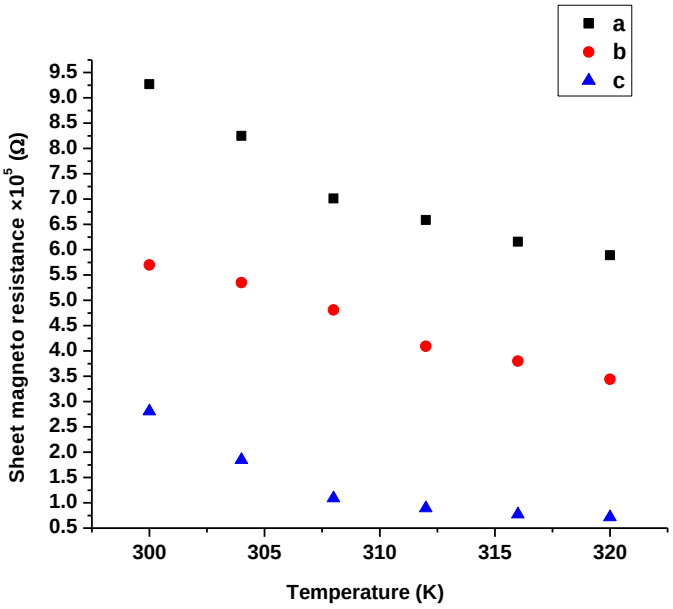

Figure 4.5: Sheet magneto resistance against temperature for CdS thin films with subject of constant magnetic field 0.55 T

In case of CdS thin films magnetic field remained constant, a magnetic field of low intensity i.e. 0.55 Tesla was applied and current was taken as 0.1 micro Ampere depending upon the electrical properties of the CdS thin film samples. During the electrical characterization of CdS thin films, temperature was ranging from 300K to 320K. For CdS thin films with different deposition time, decreasing trend of magneto resistance with increase of temperature was observed. It was also observed that with increase of deposition time which corresponded to increase of thickness, magneto resistance decreased. Higher order of magneto-resistance has been found for different deposition time of CdS samples. As

magneto resistance are found to be in order of 10^5 or $10^4$for these CdS thin films so change in resistivity for CdS thin films are more than 2 % of order of change in resistivity which shows that CdS thin films observe anisotropic magneto resistance phenomenon [35].

4.4.5 IV Characterization of CdS thin film

Ohmic and non-ohmic behavior of CdS thin film with deposition time 10 minutes under influence of light and dark conditions are shown in Figure 4.6 and Figure 4.7. Under light, there would be more generation of electron-hole pair which results in non-ohmic behavior. Four curves of different color represented four paths of voltages while applying Van der Pauw technique. Under dark condition, there would be no generation of electron-holes pair which results in ohmic behavior.

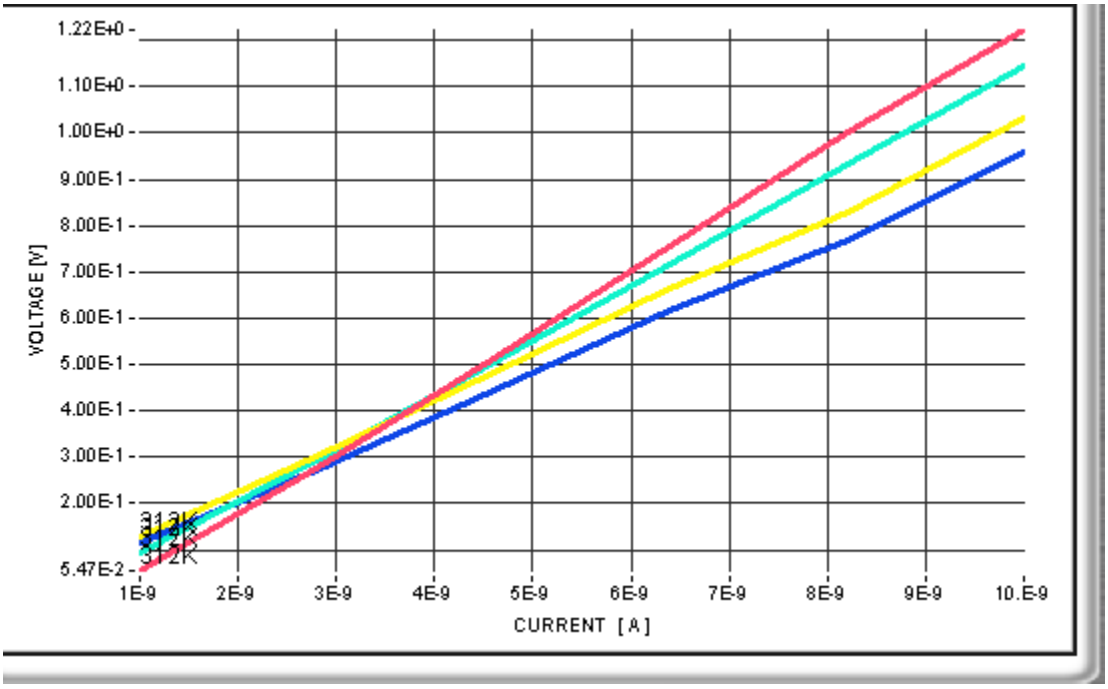

Figure 4.6: Ohmic behavior under dark condition

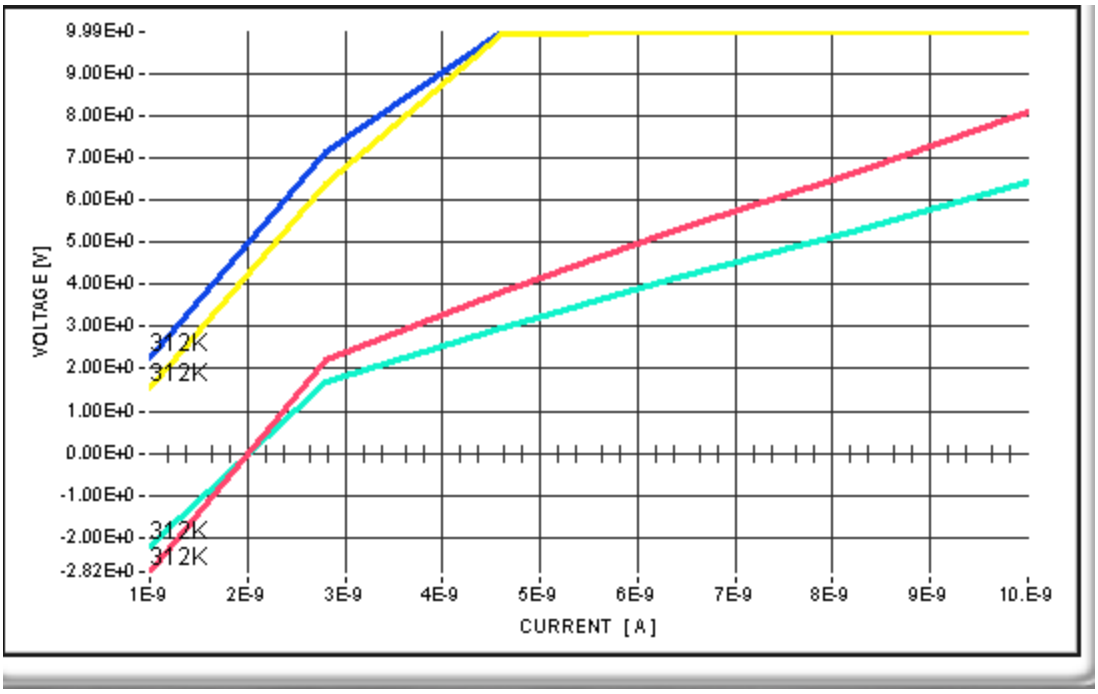

Figure 4.7: Non-ohmic behavior under influence of light

4.4.6 VRH Modeling on Cadmium sulfide thin film

The dependence of electrical conductivity upon temperature is shown in Figure 4.8 for all of these three samples. The obtained semiconductor like behavior of electrical conductivity is expressed by the relation [36]:

$$\sigma_{dc} = \sigma_0 \exp(-\Delta E / k_B T) \qquad (4.3)$$

Where σ_0 is the pre-exponential factor, ΔE is activation energy and k_B is the Boltzmann constant .Using equation 4.3, activation energy of the sample can be calculated from the slope of $\ln \sigma$ vs $1/k_B T$ plot. Obtained activation energies are 0.049 ± 0.003 eV for 248 nm, 0.12 ± 0.01 eV for 444 nm, 0.268 ± 0.011 eV for 860 nm respectively with fitting coefficient of 0.99 in all these cases.

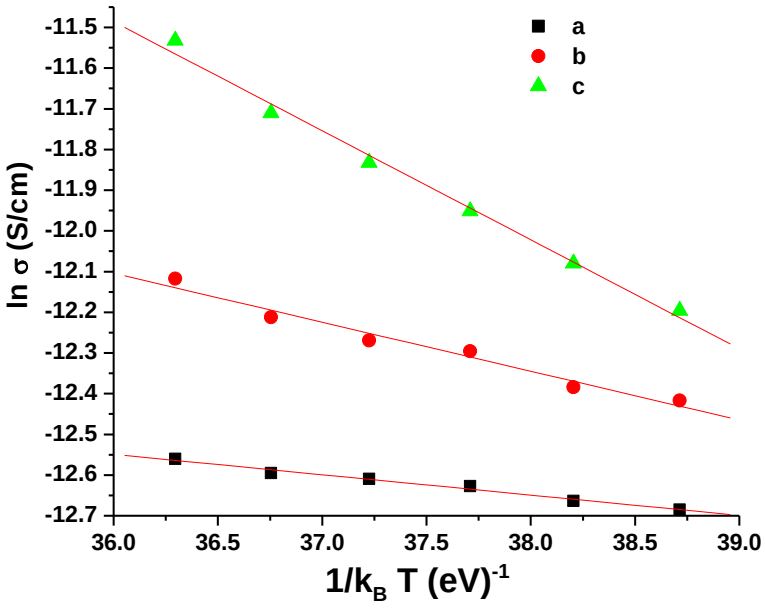

Figure 4.8: Variation of electrical conductivity with temperature

The value of pre-exponential factor σ_0 provides an identification of the fact that whether the conduction is due to extended states or is by localized states [37]. In order to conduct by extended state conduction, σ_0 must be in the range of 10^3-10^4 S/cm [38] and there should be a smaller value for the hopping conduction between localized states, in which electrons hop between one localized state to the next separated by an energy gap. In these entire three sample, the value of σ_0 lies between 10^{-3} - 10^{-1} S/cm. These values confirm that the conduction takes place by the hopping mechanism. Small values of activation energy for these three samples provide further confirmation of the hopping phenomenon [39].

In the light of the above observations, it is assumed that hopping process is governed by Mott's Variable Range Hopping (VRH) mechanism expressed as [40, 41]:

$$\sigma = \sigma_o \exp\{-(T_o/T)^{1/4}\} \qquad (4.4)$$

Where T_o is the degree of disorder expressed by $T_o = \lambda\alpha^3 / \{k_B N(E_F)\}$, $N(E_F)$ is the density of states at fermi level, λ is dimensionless constant of about 16 [41, 42] and α represents localization length of excited electron ($10^7 cm^{-1}$). Mott VRH plot for these three samples are shown in Figure 4.9.The hopping distance (R) and average hopping energy (W_{dc}) are

calculated by the following relations as a function of temperature [41], and are shown in Table 4.4.

$$R = \{9/(8\pi\alpha k_B T N(E_F))\}^{0.25} \quad (4.5)$$

$$W_{dc} = 3/(4\pi R^3 N(E_F)) \quad (4.6)$$

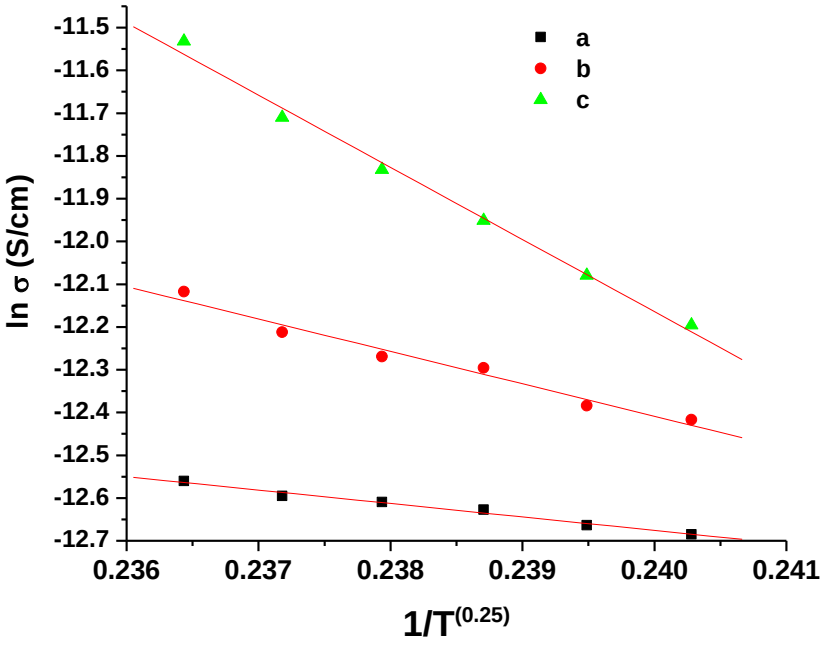

Figure 4.9: Mott's VRH plots for (a), (b) and (c) samples

It is clear from Table 4.4 the hopping distance decreases while hopping energy increases linearly with rising temperature while both of them increase with increases with thickness. The necessary conditions for applying Mott's VRH mechanism are [38]

(iii) average hopping energy must be greater than thermal energy (i.e. $W_{dc} > k_B T$) *and*

(iv) $\alpha R > 1$

Here both the conditions are satisfied in all of these three samples.

Table 4.4: Hopping Energy and Hopping distance for three CdS thin films

Sample	$N(E_F)$	R (nm)	W_{dc} (meV)
a	2.02E+20	2.88±0.05	51
b	5.81E+18	6.99±0.11	123
c	2.30E+17	15.7±0.03	277

So for the samples namely a, b, and c ,$N(E_F)$ is 2.02E+20, 5.81E+18 and 2.30E+17 respectively and R(nm) is 2.88±0.05, 6.99±0.11, 15.7±0.03 respectively while W_{dc} is 51 meV, 123meV and 277meV respectively for CdS thin films with different thickness.

4.5 Summary

CdS thin films are prepared by close space sublimation technique with different deposition time. These thin films are characterized by SEM, XRD, EDS and Ecopia Hall Effect measurement system for their morphological, structural, and electrical properties. XRD and SEM determined the crystallite size and grain size respectively. Dc electrical resistivity of CdS thin film is found to be of the order of 10^5 ohm-cm at room temperature. Decreasing trend for magneto resistance with temperature is observed, CdS thin films observe anisotropic magneto resistance phenomenon. Resistivity and sheet resistance variations with deposition time are also discussed. IV characterizations for CdS thin films under UV light and dark conditions showed different features which is responsible for many photovoltaic applications of group II-VI semiconductors. The resistivity of CdS thin films also follows the hopping model.

4.6 References

[1] H. Zhang, X. Ma, D. Yang, Mater.Lett.58 (2003) 5.

[2] R. Tenne, V. M. Nabutovsky, E. Lifshitz, A. F. Francis, Solid State Commun. 82 (1992) 651.

[3] V. Ruxandra, S. Antohe, J. Appl. Phys. 84 (1998) 727.

[4] B. Su, K. L. Choy, Thin Solid Films 102 (2000) 361.

[5] A. G. Valyomana, K. P. Vijayakumar, C. Purushothaman, J. Mater. Sci. Lett. 11 (1992) 616.

[6] H. Chavez, M. Jordan, J. C. McClure, G. Lush, V. P. Singh, J. Mater. Sci. 8 (1997) 151.

[7] F. Izci, S. Kose, K. Yckaya, Proc. Suppl. Bpl. 5 (1997) 1115.

[8] A. G. Valyomana, K. P. Vijayakumar, C. Purushothaman, J. Mater. Sci. Lett. 9 (1990) 1025.

[9] A. Al Kuhaimi, Vacuum 51 (1998) 349.

[10] J. Pantoja, X. Mathew, Solar Energy Materials & Solar Cells 76 (2003) 313.

[11] M. E. Ozsan, D. R. Johnson, M. Sadeghi, D. Svapathasundaram, G. Goodlet, M. J. Furlong, L. M. Peter, A. A. Shingleton, J. Mater. Sci. 7 (1996) 119.

[12] N. Romeo, A. Bosio, R. Dedeschi, V. Canevari, Thin Solid Films 327 (2000) 361.

[13] H. Ariza-Calderon, R. Lozada-Morales, O. Zelaya-Angel, J.G. Mendoza, L. Banos, J. Vac. Sci. Technol. 14 (1996) 2480.

[14] S.J. Ikhmayies, Production and Characterization of CdS/CdTe Thin Film Photovoltaic Solar Cells of Potential Industrial Use, Ph.D. Thesis, University of Jordan, (2002).

[15] O. Vigil, I. Riech, M. Garcia-Rocha, O. Zelaya-Angel, J. Vac. Sci. Technol. 15 (1997) 2282.

[16] O. Melo De, L. Hernan´dez, O. Zelaya-Angel, R. Lozada-Morales, M. Bercerril, E. Vasco, Appl. Phys. Lett. 65 (1994) 1278.

[17] M. Lepek, B. Dogil, Thin Solid Films 109 (1983) 103.

[18] B. Ullrich, R. Schroeder, IEEE J. Quantum Electron. 37 (2001) 1363.

[19] H. Wang, Y. Zhu, P.P. Ong, J. Cryst. Growth 220 (2000) 554.

[20] M. Khanlary, P. Townsenda, B. Ullrich, D.E. Hole, J. Appl. Phys. 97 (2005) 23512.

[21] A.Nazir, Preparation and characterization of II-VI group thin films, MS Thesis, NUST, 2010

[22] J. Santamaria, I. Martil, E. Iborra, G. G. Diaz, F. S. Queada, Solar Energy Matter 28 (1990) 31.

[23] S. N. Sahu, S. Chandra, Solar Cells, 22 (1987) 163.

[24] J. W. Orton, B. J. Goldsmith, J. A. Chapman, M. A. Powell, Appl. Phys., 53 (1982) 1602.

[25] N. A. Shah, A. K. S. Aqili, A. Maqsood, Crystal Growth 290 (2006) 452.

[26] J. P. Enrquez, X. Mathew, Solar Energy Materials & Solar Cells 76 (2003) 313.

[27] K. Ravichandran, P. Philominathan, Applied Surface Science 255 (2009) 5736.

[28] E. D. Palik, Handbook of Optical Constants of Solids II, Academic Press, San Diego, USA, (1991).

[29] J. M. Magn, Mater. 152 (1996) 159.

[30] V. Kapaklis, P. Poulopoulos, V. Karoutsos, T. Manouras, C. Politis, Thin Solid Films 510 (2006) 138.

[31] K. L. Chopra, Thin Film Phenomena, McGraw-Hill, New York (1969).

[32] Z.Ali, Fabrication of II-VI semi conductors thin films and a study of structural, optical and electrical properties, PhD Thesis, Quaid-i-Azam University, 2005

[33] B.Podor, J. Balazs, M. Harsy : phys. Stat. sol. (a) 8, 613(1971)

[34] A. Karipera, E. Genera, F. Godel, C. Humus, T. Ozpozand : Materials Chemistry and Physics 129 (2011) 183– 188

[35] Magneto Resistance Overview: Janice Nickel, Computer Peripherals Laboratory HPL-95-60, June, 1995.

[36] I.H. Gul, A.Z. Abbasi, F.Amin, M. Anis-ur-Rehman, A. Maqsood, J. Magn.Magn.Mater. 311 (2007) 494

[37] M. Fadel, A.A. Nigim, H.T Elshair, Vacuum 46 (1995) 1279.

[38] A.A. Dakhel, Cryst. Res. Technol. 41 (2006) 800-802.

[39] N.F. Mott, Philos. Mag. 22 (1970) 7.

[40] N.F. Mott, E.A. Davis, Philos. Mag. 22 (1970) 903.

[41] N.F. Mott, E.A. Davis, Electronic processes in nano crystalline materials, Clarendon, Oxford, 1979.

[42] A. Ganguly, S.K. Mandal, S. Chaudhary, A.K. Pal, J. Appl. Phys. 90 (2001) 5652.

.

CHAPTER 5

5.1 Conclusion

In the present work, "Ecopia 5000 Hall effect measurements system", has been made operational successfully for the first time at Thermal Transport Laboratory, SCME, NUST, Islamabad. This characterization tool is of great importance in industry for electrical characterization of semiconductors thin films.

ZnO and CdS thin films belong to II-VI semiconductors. These thin films are characterized electrically as a function of temperature. Electrical resistivity of ZnO thin film is found to be of the order of 10^3 ohm-cm. As Hall coefficients for ZnO films were found to be negative which indicate that ZnO thin films are of n-type with more concentration of electrons as charge carriers in comparison with the concentration of the holes. Bulk concentrations of three films of ZnO with thicknesses 860nm, 1110nm and 1510nm were found to be 1.5E18, 6E19, 2.5E20 cm^{-3} and the mobilities of these three films were found to be 16.3, 24 and 27.9 cm^2/Vs respectively which also confirmed that with the increase of the thickness, mobility of carriers improved. Decreasing trend for magneto resistance as a function of temperature was observed. The change in the resistivity of ZnO was more than 2% of the order in the change of resistivity when these films were subjected to magnetic field of 0.55 T which confirmed anisotropic magneto resistance phenomenon in ZnO semiconductor films. I-V characterizations for films under light and dark conditions showed features which is responsible for its applications in photovoltaic materials. The resistivity of ZnO thin films also follows the hopping model. Activation energies were found to be 0.03 ± 0.01 eV for 860nm, 0.157 ± 0.004 eV for 1110nm, 0.173 ± 0.007 eV for 1510nm respectively with fitting coefficient of 0.99 in all of these cases. Dc electrical resistivity of CdS thin film is found to be of the order of 10^5 ohm-cm. Hall coefficients for these as deposited CdS thin films were found to be negative which indicate that CdS thin films are of n-type. Mobility for these three CdS thin films with thickness 248nm, 444nm and 860nmwere found to be 81.3, 112.3 and 262.3 cm^2/Vs respectively and similarly bulk concentrations for the same thicknesses are found to be 7.11E14, 1.56E15 and 2.17E16 cm^{-}

^{3}respectively.Decreasing trend for magneto resistance with temperature was observed for CdS films, these films observe anisotropic magneto resistance phenomenon. IV characterizations for CdS thin films under light and dark conditions showed different features which is again responsible for many photovoltaic applications of group II-VI semiconductors like ZnO thin films. The resistivity of CdS thin films also follows the hopping model. Obtained activation energies are 0.049 ± 0.003 eV for 248nm, 0.12 ± 0.01 eV for 444nm, 0.268 ± 0.011 eV for 860nm respectively which also showed that activation energy increased with deposition time. As a result of it, different electrical features of II-VI group semi conductors under light and dark conditions showed that these II-VI semiconductors can be used in wide variety of photovoltaic applications as photovoltaic materials like in thin films photovoltaic cells and solar cells.

5.2 Future recommendations

Regarding future work, electrical characterization of other II-VI semiconductors like CdTe, ZnTe and ZnS will be studied as a function of temperature. For electrical studies at very low temperature near 80K, such electrical properties will be measured especially in case of metals thin films as a function of temperature at Ecopia HMS-5000 Hall effect measurement system using liquid nitrogen. Measurements at low temperature will show new electrical studies and add new information in the scientific literature.